OXFORD GENETICS

GENETICS, 2022, 222(1), iyac106
https://doi.org/10.1093/genetics/iyac106
Advance Access Publication Date: 25 July 2022
Investigation

Turning coldspots into hotspots: targeted recruitment of axis protein Hop1 stimulates meiotic recombination in *Saccharomyces cerevisiae*

Anura Shodhan, Martin Xaver, David Wheeler, Michael Lichten *

Laboratory of Biochemistry and Molecular Biology, Center for Cancer Research, National Cancer Institute, Bethesda, MD 20892, USA

*Corresponding author: National Cancer Institute, Building 37, Room 6124, 37 Convent Dr. MSC4260, Bethesda, MD 20892-4260, USA.
Email: michael.lichten@nih.gov

Abstract

The DNA double-strand breaks that initiate meiotic recombination are formed in the context of the meiotic chromosome axis, which in *Saccharomyces cerevisiae* contains a meiosis-specific cohesin isoform and the meiosis-specific proteins Hop1 and Red1. Hop1 and Red1 are important for double-strand break formation; double-strand break levels are reduced in their absence and their levels, which vary along the lengths of chromosomes, are positively correlated with double-strand break levels. How axis protein levels influence double-strand break formation and recombination remains unclear. To address this question, we developed a novel approach that uses a bacterial ParB-*parS* partition system to recruit axis proteins at high levels to inserts at recombination coldspots where Hop1 and Red1 levels are normally low. Recruiting Hop1 markedly increased double-strand breaks and homologous recombination at target loci, to levels equivalent to those observed at endogenous recombination hotspots. This local increase in double-strand breaks did not require Red1 or the meiosis-specific cohesin component Rec8, indicating that, of the axis proteins, Hop1 is sufficient to promote double-strand break formation. However, while most crossovers at endogenous recombination hotspots are formed by the meiosis-specific MutLγ resolvase, crossovers that formed at an insert locus were only modestly reduced in the absence of MutLγ, regardless of whether or not Hop1 was recruited to that locus. Thus, while local Hop1 levels determine local double-strand break levels, the recombination pathways that repair these breaks can be determined by other factors, raising the intriguing possibility that different recombination pathways operate in different parts of the genome.

Keywords: meiosis; meiotic recombination; double-strand breaks; chromosome axis; crossing over; Hop1; recombination pathways

Introduction

During meiosis, the diploid genome is reduced by half to form haploid gametes by the separation of homologous chromosomes of different parental origin (herein called homologs) during the first of 2 nuclear divisions (meiosis I). Faithful segregation of homologs requires that they must first identify and link with each other. This is achieved by homologous recombination, which first promotes homolog pairing and then forms crossovers (COs) that physically connect homologs and ensure their proper disjunction at meiosis I (Zickler and Kleckner 1999; Whitby 2005; Ur and Corbett 2021). Errors in homologous recombination cause aneuploidy in gametes, which in turn causes infertility, pregnancy loss, and genetic disorders (Hassold and Hunt 2001; Srivastava *et al.* 2012; Wang *et al.* 2017; Gao *et al.* 2018).

Meiotic recombination occurs in the context of a chromosome axis that contains 3 components: cohesin; an axis core protein; and HORMA domain-containing proteins (Hollingsworth and Ponte 1997; Zickler and Kleckner 1999; Blat *et al.* 2002; Glynn *et al.* 2004; Tsubouchi and Roeder 2006; Niu *et al.* 2007; Yang *et al.* 2008; Kugou *et al.* 2009; Niu *et al.* 2009; Callender and Hollingsworth 2010; Kim *et al.* 2010; Panizza *et al.* 2011; Chuang *et al.* 2012; Pyatnitskaya *et al.* 2019; Ur and Corbett 2021). The cohesin core holds the sister chromatids together and organizes them in a linear array of loops (Zickler and Kleckner 1999; Berezney *et al.* 2000; van Heemst and Heyting 2000; Hadjur *et al.* 2009; Nativio *et al.* 2009; Davidson *et al.* 2019; Kim *et al.* 2019; Golfier *et al.* 2020). Meiotic cohesin, which contains the meiosis-specific kleisin subunit Rec8, is important for most of the chromosomal localization of the other 2 axis proteins in wild-type cells (Smith and Roeder 1997; Klein *et al.* 1999; Blat *et al.* 2002; Riedel *et al.* 2006; Jin *et al.* 2009; Joshi *et al.* 2009; Katis *et al.* 2010; Panizza *et al.* 2011; Sun *et al.* 2015; Heldrich *et al.* 2020, 2022). Axis core proteins (Red1 in *Saccharomyces cerevisiae*, ASY3/4 in *Arabidopsis*, SYCP2/3 in mammals, Rec10 in *S. pombe*) have diverged considerably in sequence but have similar domain structures and are functionally conserved (Rockmill and Roeder 1990; Hollingsworth and Ponte 1997; Smith and Roeder 1997; de los Santos and Hollingsworth 1999; Lorenz *et al.* 2004; Yang *et al.* 2006; West *et al.* 2019; Ur and Corbett 2021). HORMA domain-containing proteins (Hop1 in *S. cerevisiae* and *S. pombe*, ASY1/PAIR2 in plants, HORMAD1/2 in mammals, HTP-1/2/3/HIM-3 in *C. elegans*) are also functionally conserved, and in most organisms contain a HORMA domain and a loop

Received: May 12, 2022. **Accepted:** July 01, 2022

containing a peptide sequence, called a closure motif, that binds either to its own HORMA domain to form a closed structure or to a HORMA domain on another protein to form oligomers (Hollingsworth and Byers 1989; Hollingsworth and Ponte 1997; Caryl *et al.* 2000; Woltering *et al.* 2000; Lorenz *et al.* 2004; Nonomura *et al.* 2004; Martinez-Perez and Villeneuve 2005; Yang *et al.* 2006; Baudat and de Massy 2007; Wojtasz *et al.* 2009; Kim *et al.* 2014; West *et al.* 2018). HORMA domain proteins are recruited to the axis by an interaction between their HORMA domain and a closure motif on the axis core protein (West *et al.* 2018, 2019). Although the main function of these proteins is similar in most organisms, there are also differences that have been discussed in detail elsewhere (Zickler and Kleckner 2015, 2016; Ur and Corbett 2021). For simplicity, the rest of this introduction will focus on the function of these proteins in meiotic recombination in *S. cerevisiae*.

Chromosome axis proteins are important for the first step of meiotic recombination, the formation of programmed DNA double-strand breaks (DSBs) by the meiosis-specific protein Spo11 and its co-factors: the RMM complex (Rec114, Mer2, Mei4); the MRX complex (Mre11, Rad50, Xrs2); Rec102-Rec104; and Ski8 (Malone *et al.* 1991; Bergerat *et al.* 1997; Uetz *et al.* 2000; Keeney 2001; Kee and Keeney 2002; Tesse *et al.* 2003; Arora *et al.* 2004; Kee *et al.* 2004; Prieler *et al.* 2005; Henderson *et al.* 2006; Li *et al.* 2006; Maleki *et al.* 2007; Panizza *et al.* 2011; Stanzione *et al.* 2016). On a regional scale (on the order of 20–50 kb), enrichment levels for Spo11 and DSBs are closely related to those observed for Hop1 and Red1 (Hollingsworth and Ponte 1997; Blat *et al.* 2002; Pan *et al.* 2011; Panizza *et al.* 2011; Smagulova *et al.* 2011; Sun *et al.* 2015). In addition, mutant analyses have shown that the absence of any of the axis proteins results in a reduction in DSBs, although the extent of reduction can differ between genome regions (Zickler and Kleckner 1999; Blat *et al.* 2002; Glynn *et al.* 2004; Kugou *et al.* 2009; Kim *et al.* 2010; Panizza *et al.* 2011; Ur and Corbett 2021). *hop1* mutants seem to show the most pronounced DSB reduction, at least when measured at loci where DSBs form frequently, called hotspots (Mao-Draayer *et al.* 1996; Schwacha and Kleckner 1997; Xu *et al.* 1997; Woltering *et al.* 2000; Peciña *et al.* 2002; Niu *et al.* 2005). Hop1 is thought to promote DSB formation by interacting with Mer2, a member of the trimeric RMM complex, and this interaction is conserved in other species (Stanzione *et al.* 2016; Kariyazono *et al.* 2019; Claeys Bouuaert *et al.* 2021; Rousová *et al.* 2021). Mer2, in turn, interacts with the other RMM components as well as other proteins that are important for Spo11-mediated DSB formation (Acquaviva *et al.* 2013; Sommermeyer *et al.* 2013; Rousová *et al.* 2021). *In vitro* studies indicate that although Red1 has no detectable affinity for Mer2, Red1 stimulates Hop1-Mer2 interaction by changing Hop1's conformation and increasing its affinity for Mer2 (Rousová *et al.* 2021). Hop1 is also required for cohesin-independent enrichment of Red1 in certain parts of the genome (Panizza *et al.* 2011; Sun *et al.* 2015; Heldrich *et al.* 2020). Taken together, these observations suggest that Hop1 may be the primary axis protein promoting DSB formation, although this has not been directly demonstrated.

Once DSBs form, Hop1 and Red1 play subsequent roles in promoting interhomolog recombination and in promoting CO formation. DSBs promote Hop1 phosphorylation by the Mec1 (ATR) and Tel1 (ATM) kinases (Carballo *et al.* 2008), and this promotes use of the homolog rather than the sister chromatid as a repair template (Hollingsworth and Ponte 1997; Tsubouchi and Roeder 2006; Niu *et al.* 2007, 2009; Callender and Hollingsworth 2010; Chuang *et al.* 2012). Once paired, homologs are held together by a tripartite proteinaceous structure called the synaptonemal complex and Hop1 is removed from the chromosome axis, curbing further DSB formation and removing the inter-sister recombination barrier to allow quick repair of any remaining breaks (Borner *et al.* 2008; Joshi *et al.* 2009; Wojtasz *et al.* 2009; Zanders and Alani 2009; Goldfarb and Lichten 2010; Daniel *et al.* 2011; Kauppi *et al.* 2013; Thacker *et al.* 2014; Lambing *et al.* 2015; Subramanian *et al.* 2016, 2019). Red1 interacts with Zip4 (Yang *et al.* 2008; De Muyt *et al.* 2018; Pyatnitskaya *et al.* 2019), a member of the ZMM protein ensemble (Zip1, Zip3, the Zip2-Zip4-Spo16 complex, the Msh4-Msh5 complex, and Mer3) that stabilizes double-Holliday junction intermediates and directs them toward resolution as COs by the meiosis-specific resolvase, MutLγ (Mlh1-Mlh3 and Exo1; Schwacha and Kleckner 1994; Wang *et al.* 1999; Khazanehdari and Borts 2000; Kirkpatrick *et al.* 2000; Tsubouchi and Ogawa 2000; Allers and Lichten 2001a, 2001b; Hoffmann *et al.* 2003; Bishop and Zickler 2004; Borner *et al.* 2004; Jessop *et al.* 2006; Lynn *et al.* 2007; Nishant *et al.* 2008; Zakharyevich *et al.* 2010; Comeron *et al.* 2012; Wang *et al.* 2012; Yang *et al.* 2012; Al-Sweel *et al.* 2017; De Muyt *et al.* 2018; Pyatnitskaya *et al.* 2019; Cannavo *et al.* 2020; Kulkarni *et al.* 2020; Sanchez *et al.* 2020). This is the major pathway for CO formation; a minority of COs are formed by the mitotic structure-selective nucleases (SSNs) Mus81-Mms4, Slx1-Slx4, Yen1 (de los Santos *et al.* 2003; Argueso *et al.* 2004; Hollingsworth and Brill 2004; Lynn *et al.* 2007; Jessop and Lichten 2008; De Muyt *et al.* 2012; Zakharyevich *et al.* 2012; Agostinho *et al.* 2013; Oke *et al.* 2014). Joint molecule resolution and CO formation in both pathways depend on the meiosis-specific transcription factor Ndt80, which drives the mid-meiosis expression of many proteins required to complete meiosis and sporulation, including the polo-like kinase Cdc5 that stimulates resolvase activities (Xu *et al.* 1995; Chu and Herskowitz 1998; Allers and Lichten 2001a; Clyne *et al.* 2003; Sourirajan and Lichten 2008; Matos *et al.* 2011; De Muyt *et al.* 2012; Sanchez *et al.* 2020).

In summary, meiotic axis proteins play roles in various stages of meiotic recombination, with current data indicating that Hop1 has an early role in DSB formation and partner choice, while Red1 has a later role in recombination pathway choice. However, because Red1 and Hop1 are codependent for much of their localization, determining the specific role that each protein plays in meiotic recombination remains a challenge. Here, we used a novel approach based on a bacterial ParB-*parS* partition system (Khare *et al.* 2004; Dubarry *et al.* 2006; Murray *et al.* 2006; Sullivan *et al.* 2009; Graham *et al.* 2014; Attaiech *et al.* 2015), to recruit Hop1 to regions where meiotic axis proteins are normally depleted. We find that recruiting Hop1 at high levels is sufficient to dramatically increase both DSBs and homologous recombination, consistent with Hop1 being the most immediate determinant of where meiotic recombination occurs in the genome.

Materials and methods

Yeast strains

All *S. cerevisiae* strains (Supplementary File 1, sheet 1) used in this study are of SK1 background (Kane and Roth 1974) and were made by transformation or genetic crosses. To monitor the effect of axis protein recruitment via the ParB-*parS* system, 2 recombination reporter inserts were used (for schematics, see Figs. 2a and 9a). The first is a modification of the previously described *URA3-ARG4-pBR322* insert (Wu and Lichten 1995; Borde *et al.* 1999), and the second a modification of the previously described *URA3-tel-ARG4* insert (Jessop *et al.* 2005; Ahuja *et al.* 2021). For both inserts, a 1-kb fragment containing the *parSc2* element from chromosome *c2* of *Burkholderia cenocepacia* J231 (Saad *et al.* 2014)

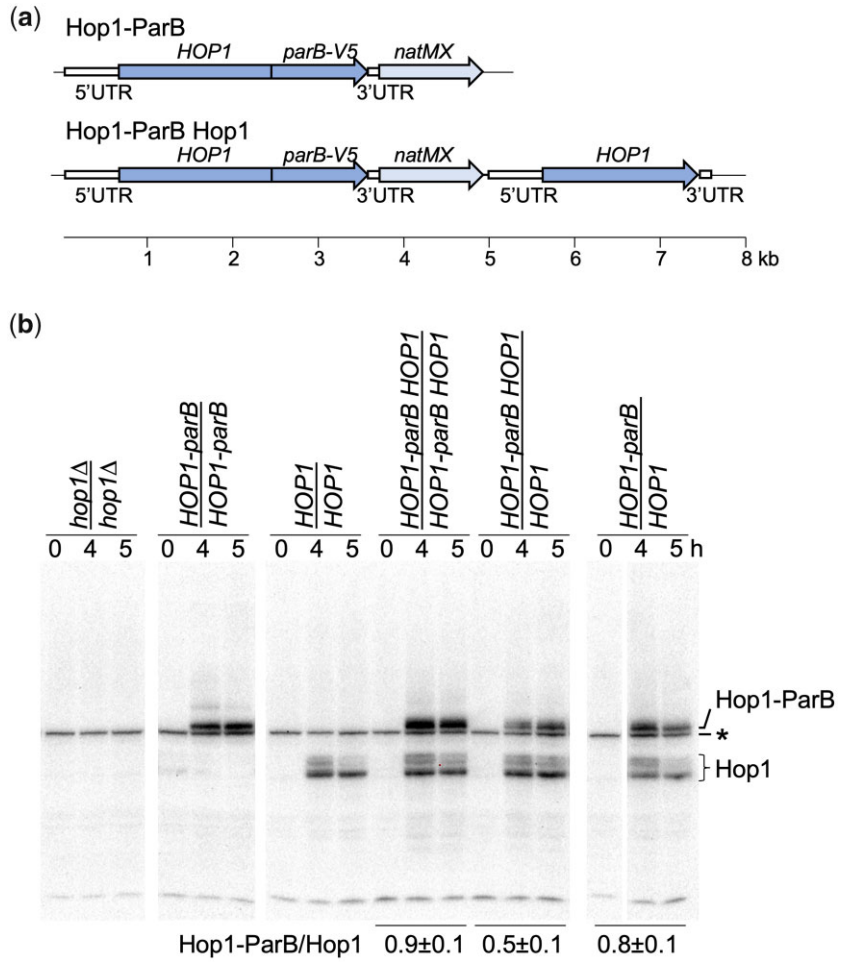

Fig. 1. ParB fusion constructs. a) Illustration of protein fusions used. Dark arrows—coding sequences of tagged and untagged *HOP1*; vertical lines—fusion junction; light arrows—*natMX6* drug resistance cassette; open boxes—5′ and 3′ *HOP1* untranslated regions; thin black lines—flanking yeast chromosome sequences. b) Western blot of samples taken at indicated time in meiosis, probed with anti-Hop1. Bands corresponding to Hop1 and to Hop1-ParB are indicated; asterisk indicates nonspecific background band. Ratios of Hop1-ParB/Hop1 are indicated for strains where the 2 proteins are both present. See also Supplementary File 1, sheet 14.

was synthesized and added downstream of the *ARG4* gene. The *URA3-ARG4-pBR322-parS* construct was linearized by *EcoRI* and inserted 237 nt downstream of *HXT1* and 150 nt downstream of *YCR017c* by ends-out 3-piece transformation (primers in Supplementary File 1, sheet 2). For insertion at *URA3*, the construct was linearized by *ApaI*, which cuts in the *URA3* gene, and was inserted via ends-in 1-piece transformation. Hop1-ParB fusions are illustrated in Fig. 1a. The *URA3-tel-ARG4-parS* construct was inserted by ends-out transformation with a PCR-amplified copy with 60 nt termini homologous to *URA3*-flanking sequences (primers in Supplementary File 1, sheet 2). Sequences encoding ParBc2, which binds to *parSc2* (Saad *et al.* 2014), were modified to include a V5 tag (Funakoshi and Hochstrasser 2009) and a stop codon at its C-terminus. This was combined with *HOP1* flanking sequences in the following order to make pMJ1088 (sequence in Supplementary File 3): the *HOP1* promoter (+652 to −1 nt); ParBc2-V5—stop codon; *HOP1* 3'UTR (131 bp starting at the 3′ end of *HOP1* coding sequences); *natMX4* (Lorenz 2015). PCR products (primers in Supplementary File 1, sheet 2) containing this element were integrated at *HOP1* by single ends-in transformation to produce a *HOP1* duplication where 1 copy was C-terminally tagged *[HOP1-parBsc2-V5]-natMX-HOP1*, and by ends-out replacement transformation to produce a single C-terminally tagged copy of *HOP1* (*[HOP1-parBsc2-V5]-natMX*). Although both *HOP1-V5-parBsc2* and *HOP1* are expressed from the endogenous *HOP1* promoter, levels of the Hop1-V5-ParB fusion protein were about 10–20% lower than of the corresponding wild-type Hop1 protein (Fig. 1b and Supplementary File 1, sheet 14).

To genetically monitor CO, markers flanking the *URA3-arg4-pBR322-parS* insert at *URA3* were inserted by transformation (primers in Supplementary File 1, sheet 2): *kanMX6* (Lorenz 2015) into the intergenic region between *RIP1* and *YEL023c* ∼14 kb to the right of the insert; and *hygMX6* (Saad *et al.* 2014) into the intergenic region between *NPP2* and *EDC3* ∼11 kb to the left.

Sporulation, DNA extraction, and Southern blots

Strains were grown in liquid presporulation medium and transferred to liquid sporulation medium as described (Goyon and Lichten 1993). Culture samples were collected and processed as described (Allers and Lichten 2000; Jessop *et al.* 2005, 2006). DNA was extracted as described (Goyon and Lichten 1993), digested with the appropriate restriction enzymes, displayed on agarose gels, transferred to membranes, hybridized to radioactive probes (Supplementary File 1, sheet 3), and analyzed as described (Wu and Lichten 1994, 1995; Allers and Lichten 2001b).

Western blots

Protein was extracted from meiotic cultures, displayed on polyacrylamide gels, blotted to membranes and probed basically as described (Kaur *et al.* 2018), except that 5% nonfat dry milk was used in place of iBlock. Primary antisera and dilutions used were: rabbit anti-Hop1 (made for this work, 1:75,000) and goat anti-Arp7 (Santa Cruz Biotechnology Cat# sc-8961, RRID: AB_671730, 1:1,000). Secondary antisera were: goat polyclonal anti-rabbit conjugated with alkaline phosphatase (Abcam Cat# ab97048, RRID: AB_10680574, 1:10,000) and rabbit anti-goat IgG conjugated with alkaline phosphatase (Sigma-Aldrich Cat# A4187, RRID: AB_258141, 1:5,000). Chemiluminescence signals were captured using a BioRad Chemidoc MP imaging system and were quantified using the gel quantification tools in Fiji (Schindelin *et al.* 2012).

Cytology

Nuclear divisions were monitored by DAPI staining as described (Goyon and Lichten 1993). Meiotic chromosome spreads and staining with antisera were performed as described (Loidl *et al.* 1991). The primary antibodies were: rabbit polyclonal anti-Hop1 serum (prepared for this project), 1:7,500 and mouse anti-V5 (Bio-Rad Cat# MCA1360, RRID: AB_322378, 1:250). The secondary antibodies were: goat anti-rabbit conjugated to Alexa 488 (Molecular Probes, Cat# A-11034, RRID: AB_2576217, 1:350) and donkey anti-mouse conjugated to Cy3 (Jackson ImmunoResearch Labs Cat# 715-165-151, RRID: AB_2315777, 1:500). Images were taken on a Zeiss Axioplan 2 imaging microscope using a 100× plan apochromat objective (440782-9902) and a Zeiss AxioCam HRm camera.

Genetic analysis

Frequencies of recombination between heteroalleles were determined by random spore analysis as described (Lichten *et al.* 1987). Map distances were determined by tetrad dissection, using the formula of Perkins (Perkins 1949) as implemented at https://elizabethhousworth.com/StahlLabOnlineTools/compare2.php.

Calibrated chromatin immunoprecipitation and sequencing

Chromatin immunoprecipitation and sequencing (ChIP-seq) experiments used a protocol that combined and modified previous methods (Murakami and Keeney 2014; Makrantoni *et al.* 2019; Murakami H, personal communication). Strains used contained the *URA3-tel-ARG4-parS* reporter construct inserted at *URA3*. Samples taken at 0, 3, and 4 h postmeiotic induction were fixed with 1% formaldehyde for 30 min at room temperature and quenched with 125 mM glycine. The cells were washed in 1× TBS (20 mM Tris–HCl, pH 7.5, 136 mM NaCl) and stored as a pellet at −80°C. *Saccharomyces mikatae* cells were similarly fixed 4 h postmeiotic induction and aliquots were frozen that contained about 1/10th the number of cells taken for *S. cerevisiae*. Both pellets were mixed in 500 µl lysis buffer (50 mM Hepes-KOH pH 7.5, 140 mM NaCl, 1 mM EDTA, 1% Triton X-100, 0.1% sodium deoxycholate, 1× Complete Protease Inhibitor Cocktail EDTA free [Roche, #04693132001], 7 µg/ml aprotinin [Thermo Scientific, #78432], 1 mM PMSF) and lysed in a Mini-Beadbeater-16 (Biospec products) for 7 cycles of 1 min on, 2 min off (where the samples were kept on ice). The lysate was sonicated using a Biorupter 300 (Diagnode) for 2 rounds of 11 cycles of 30 s on/30 s off, with a 20-min incubation on ice between the 2 rounds of sonication. Debris was then removed by centrifugation (21,130 × g, 5 min, 4°C) and another round of 11 cycles of sonication was performed. Lysates were precleared by incubating with 50 µl protein G-conjugated Dynabeads (Invitrogen, #100.04D; beads were washed twice with 1 ml lysis buffer before use) for 1 h on a rotator at 4°C. Beads were removed, and a 10-µl sample of the lysate was mixed with 190 µl TE/1%SDS (10 mM TRIS, 1 mM EDTA, 1% SDS pH7.5) and stored at 4°C to be used as input DNA. Three microliters of anti-Hop1 serum was added to the remaining lysate, which was then incubated for 3 h at 4°C with rotation. Protein G-conjugated Dynabeads (50 µl, washed twice with 400 µl 137 mM NaCl, 2.7 mM KCl, 10 mM Na_2HPO_4, 1.76 mM KH_2PO_4, pH 7.4 with 5 mg/ml bovine serum albumin) were added and the mixture was incubated overnight at 4°C with rotation. Beads were then washed twice with 1 ml of the following 3 buffers in succession; lysis buffer, wash buffer I (10 mM Tris–HCl, pH 8, 250 mM LiCl, 360 mM NaCl, 0.5% Na-deoxycholate, 1 mM EDTA, 0.5% Triton X-100), wash buffer II (10 mM Tris–HCl, pH 8, 250 mM LiCl, 0.5% Na-deoxycholate, 1 mM EDTA, 0.5% Triton X-100); for 5 min each on a rotator at 4°C. The beads were washed once with 1 ml TE wash buffer (10 mM Tris–HCl pH 8, 1 mM EDTA, 0.5% Triton X-100) at 4°C for 5 min with rotation. DNA was eluted in 40 µl elution buffer (50 mM Tris–HCl pH 8, 10 mM EDTA, 1% SDS) at 65°C for 15 min and added to a tube containing 160 µl of TE/1%SDS. Two hundred microliters of ChIP and input DNA were incubated overnight at 65°C in the presence of 1 µl RNAse (0.5 mg/ml) to reverse cross-links. A total of 7.5 µl of proteinase K (20 mg/ml) was added to each tube and incubated at 50°C for 2 h. DNA was purified using a QIAquick PCR purification kit (Qiagen, #28104) and eluted in 50 µl water. A total of 15 ng of ChIP and input DNA were used to generate libraries using NEBNext Ultra II DNA Library Prep Kit for Illumina (New England Biolabs, #E7645) and NEBNext Multiplex Oligos for Illumina (96 Unique Dual Index Primer Pairs, New England Biolabs, #E6440). Sequencing was performed with an Illumina NextSeq 550 with the NextSeq 500/550 High Output Kit v2.5 (75 Cycles).

ChIP-seq data were calibrated as described (Makrantoni *et al.* 2019). Briefly, single-ended fastq format sequences derived from ChIP-seq data were quality trimmed using fastp (Chen *et al.* 2018). Trimmed fastqs from both IP and input were aligned separately to the *SK1* target genome (Yue *et al.* 2017, available at https://yjx1217.github.io/Yeast_PacBio_2016/data/) which had been modified to reflect the genotype of the diploid MJL4236/7 (Supplementary File 1, sheet1) and also to the *S. mikatae* IFO 1815 (Kellis *et al.* 2003) spike-in control genome using minimap2 (Li 2018). Reads that did not map to SK1 were subsequently aligned to *S. mikatae* and vice versa to identify those reads that mapped to both genomes and those that mapped uniquely to a single genome. A calibration factor, called the occupancy ratio (OR), was then calculated from the counts of such reads as:

$$OR = (ipSK1/inSK1)/(ipSMIK/inSMIK) \quad (1)$$

where ipSK1 is the count of IP reads mapping uniquely to the SK1 genome, inSK1 is the count of input reads mapping uniquely to the SK1 genome, ipSMIK is the count of IP reads mapping uniquely to the *S. mikatae* genome, and inSMIK is the count of input reads mapping uniquely to the *S. mikatae* genome.

Calibrated depths for reads mapping uniquely to the SK1 genome were determined by multiplying read depths per million mapped reads by the OR computed in Equation (1). Data processing was performed on the NIH HPC Biowulf cluster (http://hpc.nih.gov). Scripts implementing the calibrated ChIP processing pipeline as a Snakemake (Mölder *et al.* 2021) workflow, suitable

for parallel execution on the Biowulf cluster, are included in Supplementary File 2; sequence reads are available at GEO, accession GSE201240.

Data representation

All values reported in figures are the mean of 2 or more independent experiments. Error bars denote the range in data values, except in Fig. 8b, where they denote calculated standard error.

Results

To recruit axis proteins to target loci, we used the bacterial ParB-*parS* chromosome segregation system, where the ParB protein binds to a <1-kb-long cluster of *parS* sites and then spreads to adjacent DNA (Lin and Grossman 1998; Dubarry *et al.* 2006; Breier and Grossman 2007; Attaiech *et al.* 2015; Soh *et al.* 2019). This system allows recruitment of multiple copies of ParB, fused to a protein of interest, with minimal disruption of chromosome integrity and function (Dubarry *et al.* 2006; Saad *et al.* 2014). We fused ParB and a V5 epitope tag to the C-terminus of Hop1 (hereafter called Hop1-ParB; Fig. 1a) to target this protein to 3 loci: *URA3*; *HXT1*; and *YCR017c*. All 3 are in regions of the yeast genome with low levels of occupancy by meiotic axis proteins and low levels of meiotic DSBs (Supplementary Fig. 1; Pan *et al.* 2011; Panizza *et al.* 2011).

Recruiting Hop1 increases meiotic recombination

To determine the effect of recruiting Hop1 on meiotic recombination, we initially used random spore analysis to examine recombination between *arg4* heteroalleles in a *URA3-ARG4-pBR322-parS* recombination reporter inserted at *URA3* (Fig. 2a). The same insert, but without *parS*, forms DSBs and undergoes recombination at levels that are location-dependent and that reflect underlying recombination levels in the region where it is inserted (Borde *et al.* 1999). As a no-insert control, we also measured recombination between heteroalleles at *LEU2* (Fig. 2a). Initial experiments used a *HOP1* gene duplication that contained both a tagged and a wild-type copy, to ensure normal function in the event that the tagged protein was only partially functional.

Recruiting Hop1-ParB caused a striking increase in recombination in the *arg4* gene inserted at *URA3* (Fig. 2b and Supplementary File 1, sheet 4). Inserts at *HXT1* and *YCR017c*, 2 other axis protein/DSB coldspots (Supplementary Fig. 1), also displayed markedly increased Arg+ recombinant frequencies when Hop1-ParB was present (Fig. 2c). The presence or absence of a ParB-tagged axis protein did not markedly change recombination frequencies at the *leu2* control locus (ranging from 3.1×10^{-3} to 4.5×10^{-3} across all crosses; Fig. 2, b and c and Supplementary File 1, sheet 4). These results suggest that levels of Hop1 in a region might be sufficient to determine levels of meiotic recombination in that region.

Recruiting Hop1-ParB also markedly increased crossing-over in a region containing the insert at *URA3*. Crossing-over was measured by analysis of tetrads from a diploid that contained a *kanMX6* insert 14-kb centromere proximal to *URA3-ARG4-pBR322-parS* in 1 parent, and a *hygMX6* insert 11-kb centromere distal in the other parent. The genetic distance for this ~35-kb interval was 12.3 ± 1.78 cM in diploids lacking Hop1-ParB and 66.2 ± 6.16 cM in diploids expressing Hop1-ParB, a ~5-fold stimulation of crossing-over (Supplementary File 1, sheet 10, also see Fig. 8). This remarkably high level of crossing-over indicates that most cells undergo recombination at this locus.

Recruiting Hop1 increases DSB formation

To confirm that recruiting Hop1 increases meiotic recombination by increasing levels of DSBs, we determined cumulative DSB levels in *sae2*Δ mutants, which accumulate unrepaired DSBs with unresected ends (Keeney and Kleckner 1995; Prinz *et al.* 1997). Consistent with previous data (Borde *et al.* 1999; Pan *et al.* 2011), very few DSBs were present in reporter inserts at the 3 target loci (*URA3*, *HXT1*, and *YCR017c*) in the absence of Hop1-ParB or when ParB alone was expressed. The presence of Hop1-ParB increased DSBs in the reporter construct dramatically at all 3 loci (Fig. 3, a and b and Supplementary File 1, sheet 5), while the DSBs at the *ARE1* control locus (Goldway *et al.* 1993) were relatively unchanged (Fig. 3b). Hop1-ParB recruitment caused the greatest increase in DSBs in the insert at *URA3* locus, where DSB levels (~21% of chromatids) are consistent with most cells experiencing a break at this locus.

We also asked if Hop1 levels affect DSBs in *cis* or *trans*. In strains with *parS* on only 1 of the 2 homologs, the homolog with *parS* displayed insert DSBs at levels like those seen in a *parS*-homozygous diploid, while the homolog lacking *parS* displayed DSBs at levels like those seen in strains without *parS* (Fig. 3, c and d and Supplementary File 1, sheet 6). Thus, the DSB increase observed is primarily due to recruited Hop1 acting in *cis*.

Hop1-ParB-stimulated DSBs require Spo11 but not Rec8 or Red1

According to current models, DSBs are formed by the Spo11 complex, which is recruited to the cohesin-based axis by interactions with Hop1, which in turn can be recruited to the axis via interactions with Red1 (Panizza *et al.* 2011; Sun *et al.* 2015; Zickler and Kleckner 2015; West *et al.* 2019; Rousová *et al.* 2021). This suggests that artificially recruiting Hop1 to chromosomes might bypass the need for Red1 or cohesin in DSB formation. To test this suggestion, DSBs in the insert at *URA3* were examined in *sae2*Δ strains that were lacking Spo11, Red1, or the meiosis-specific cohesin component Rec8.

As expected, DSBs were abolished at all loci in *spo11*Δ strains, regardless of whether Hop1-ParB was present (Fig. 4, a and b and Supplementary File 1, sheet 5). Consistent with previous reports (Woltering *et al.* 2000; Peciña *et al.* 2002; Niu *et al.* 2005), *red1*Δ mutants displayed a substantial decrease (to ~40% of wild-type controls) in DSBs at the *ARE1* control locus regardless of whether Hop1-ParB was present or absent. When only Hop1 was present, the *parS* insert locus showed a similar decrease in DSBs. However, when Hop1-ParB was present, DSB levels at the *parS* insert in *red1*Δ strains were similar to those in *RED1* strains (Fig. 4, a and b and Supplementary File 1, sheet 5). Thus, direct recruitment of Hop1 appears to bypass the role of Red1 in DSB formation.

Previous studies have shown that *rec8*Δ strains display rearranged patterns of Red1, Hop1, and Spo11-complex components, with a tendency toward reducing occupancy at hotspots in the centers of large chromosomes while preserving occupancy, albeit at much-reduced levels, on short chromosomes and at certain loci on other chromosomes (Kugou *et al.* 2009; Panizza *et al.* 2011; Sun *et al.* 2015; Heldrich *et al.* 2022). Consistent with previous data showing that, at *URA3* and *ARE1*, occupancy by these proteins is not substantially altered in *rec8*Δ mutants (Kugou *et al.* 2009; Panizza *et al.* 2011), DSBs at the *parS* insert locus and at the *ARE1* control locus were similar in *REC8* and in *rec8*Δ strains, regardless of the presence or absence of Hop1-ParB (Fig. 4, a and b and Supplementary File 1, sheet 5). Thus, unlike many DSB hotspots in the centers of long chromosomes, the hotspot created by

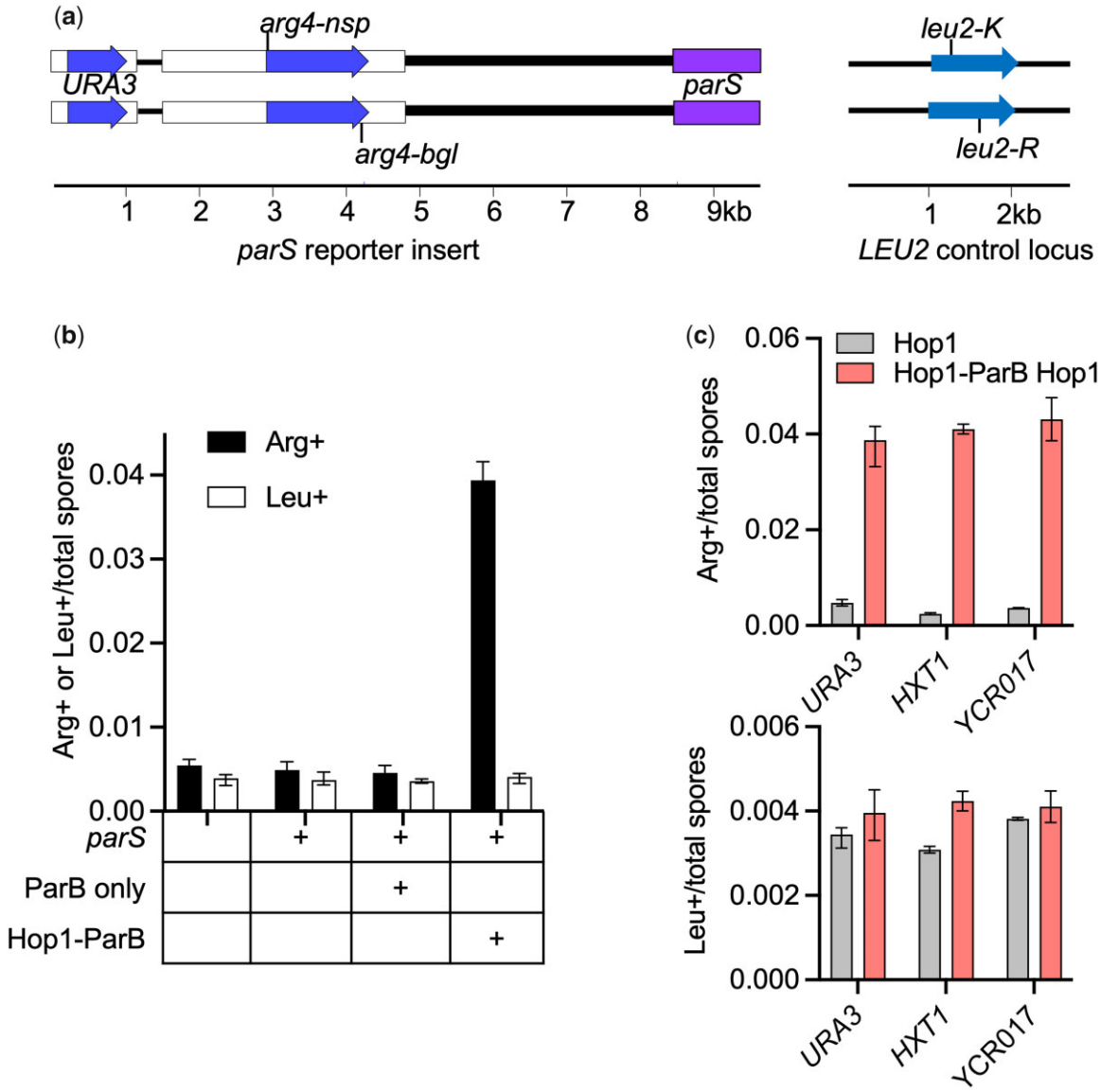

Fig. 2. Hop1 recruitment stimulates meiotic recombination. a) Left—schematic of the *URA3-ARG4-pBR322-parS* reporter insert, showing *arg4-nsp* and *arg4-bgl* heteroalleles; right—*leu2* control locus with heteroalleles. Blue—coding sequences; open boxes—yeast chromosomal sequences; filled box—*parSc2* sequences; thick line—pBR322 sequences. b) Frequencies of Arg+ (insert, black) and Leu+ (control, white) recombinants for the insert at *URA3* as shown in (a). Fusion proteins expressed are indicated; all strains also expressed wild-type Hop1. c) Frequencies of Arg+ (top) and Leu+ (bottom) recombinants in strains with inserts at the indicated locus, expressing only Hop1 (gray) or both Hop1-ParB and Hop1 (salmon). Values in graphs are the average of 2 or more independent experiments; error bars denote range. See also Supplementary File 1, sheet 4.

recruitment of Hop1-ParB to the insert at *URA3* is not affected by loss of Rec8-cohesin.

The ParB-parS system specifically enriches Hop1 at the target locus

To confirm that the ParB/*parS*-dependent increase in meiotic recombination was associated with recruitment of Hop1, we used calibrated ChIP-seq to map Hop1 occupancy genome-wide, using a spike-in sample from meiotic cells of *S. mikatae*. *S. mikatae* is substantially diverged from *S. cerevisiae* (24% nucleotide divergence genome wide), but *S. mikatae* Hop1 shows 86.5% amino acid identity with *S. cerevisiae* Hop1, and cross-reacts with the antiserum against *S. cerevisiae* Hop1 used here for ChIP (Kellis *et al.* 2003; Dujon 2006; Liti *et al.* 2013; Lam and Keeney 2015; data not shown). Strains expressing either both Hop1 and Hop1-ParB (*HOP1-ParB HOP1/HOP1*) or Hop1 alone displayed similar Hop1 occupancy profiles genome-wide (Fig. 5, a and b and Supplementary Fig. 2). However, in strains expressing Hop1-ParB, Hop1 occupancy in a ~50-kb region surrounding the *parS* insert at *URA3* was much greater than the Hop1 signal in the rest of the genome (Fig. 5, a and c). Quantitative interpretation of this pattern is complicated by the fact that strains expressing both Hop1-ParB and Hop1 have 3 modes of Hop1 chromosome binding: direct binding of the ParB domain in Hop1-ParB to chromosomal DNA; indirect binding of Hop1 through its interactions with itself and with Red1 and cohesin (Smith and Roeder 1997; Klein *et al.* 1999; Blat *et al.* 2002; Riedel *et al.* 2006; Panizza *et al.* 2011; Sun *et al.* 2015; West *et al.* 2018, 2019); and possible direct binding of Hop1 to DNA (Kironmai *et al.* 1998; Kshirsagar *et al.* 2017; Heldrich *et al.* 2020, 2022). Hop1 bound in these 3 modes is likely to be crosslinked to DNA with different efficiencies. Therefore, while the increased Hop1 ChIP signal in the vicinity of *parS* almost

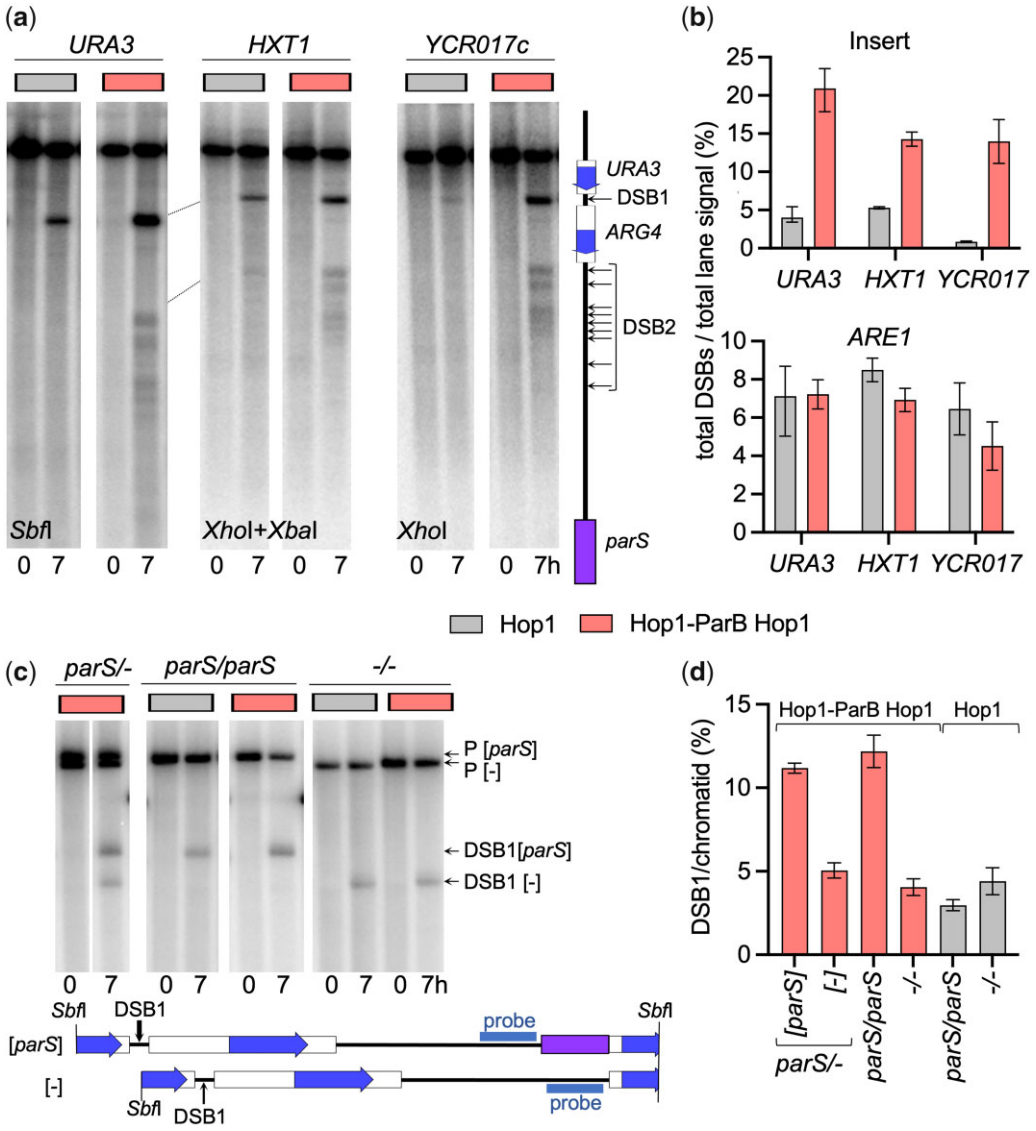

Fig. 3. Hop1-ParB recruitment increases DSBs in reporter inserts. a) Southern blot of DNA from *sae2*Δ strains, which form DSBs but do not resect or repair them, with *parS* insert at indicated locus. Indicated restriction digests were probed with *parS* sequences to detect DSBs in the insert. These occur in pBR322 sequences on either side of *ARG4* sequences (Wu and Lichten 1995), and will be called DSB1 and DSB2 as shown in the schematic. Strains were homozygous either for *HOP1* (gray) or *HOP1-parB HOP1* (salmon). b) Hop1-ParB increases DSBs (DSB1 + DSB2) at all 3 insert loci (top), but not at the *ARE1* control locus (bottom). c) Hop1-parB acts primarily in *cis:* Southern blot with DNA from a *sae2*Δ strain with inserts at *URA3* on both homologs, where: *(parS/-)*—one contains *parS* and the other does not; *(parS/parS)*—both contain *parS*; *(-/-)*—both are without *parS*. DNA was digested with *SbfI* and probed with pBR322 sequences, which allows distinction between breaks at DSB1 on chromosomes with and without *parS*. Breaks at DSB2 cannot be resolved. d) Quantification of breaks at DSB1 in the *parS* hemizygous strain, as well as in control strains with homozygous inserts where both homologs either lacked or contained *parS*. DSB1 levels are normalized on a per chromatid basis. Because of overlapping signal, signals of DSB2 on chromosomes with *parS* could not be resolved from those on chromosomes without *parS*. Values in graphs are the average of 2 or more independent experiments; error bars denote range. See also Supplementary Fig. 3 and File 1, sheets 5 and 6.

certainly indicates that more Hop1 is bound in this region, the quantitative extent of that increase remains to be determined.

We also compared the distribution of Hop1 and Hop1-ParB on chromosome spreads of cells at the pachytene stage, using anti-Hop1 to detect both proteins and anti-V5 to specifically detect the Hop1-ParB fusion protein (Fig. 5d). Cells expressing Hop1 alone displayed a pattern of lines and punctate foci, as has been previously reported (Smith and Roeder 1997). Cells expressing both Hop1 and Hop1-ParB displayed a similar pattern, and similar staining patterns were obtained with anti-Hop1 (detecting Hop1 and Hop1-ParB) and anti-V5 (detecting Hop1-ParB only). Thus, Hop1-ParB appears to localize across the genome, at least when Hop1 is also present.

Hop1-ParB provides partial Hop1 function

The experiments described above used strains with a wild-type copy of the *HOP1* gene in addition to the *HOP1-ParB* fusion (see *Materials and methods*). To determine whether Hop1-ParB was fully functional when expressed on its own, we examined meiotic spore viability, recombination, and DSB formation in strains containing a *parS* insert at *URA3* where the only source of Hop1 was a Hop1-ParB fusion (Fig. 6). In strains where only Hop1-ParB was expressed (*HOP1-parB/HOP1-parB*), spore viability was reduced to about 50% of wild type, and spore inviability patterns in tetrads were consistent with meiosis I nondisjunction (Fig. 6a and Supplementary File 1, sheet 7). Recombination between *arg4*

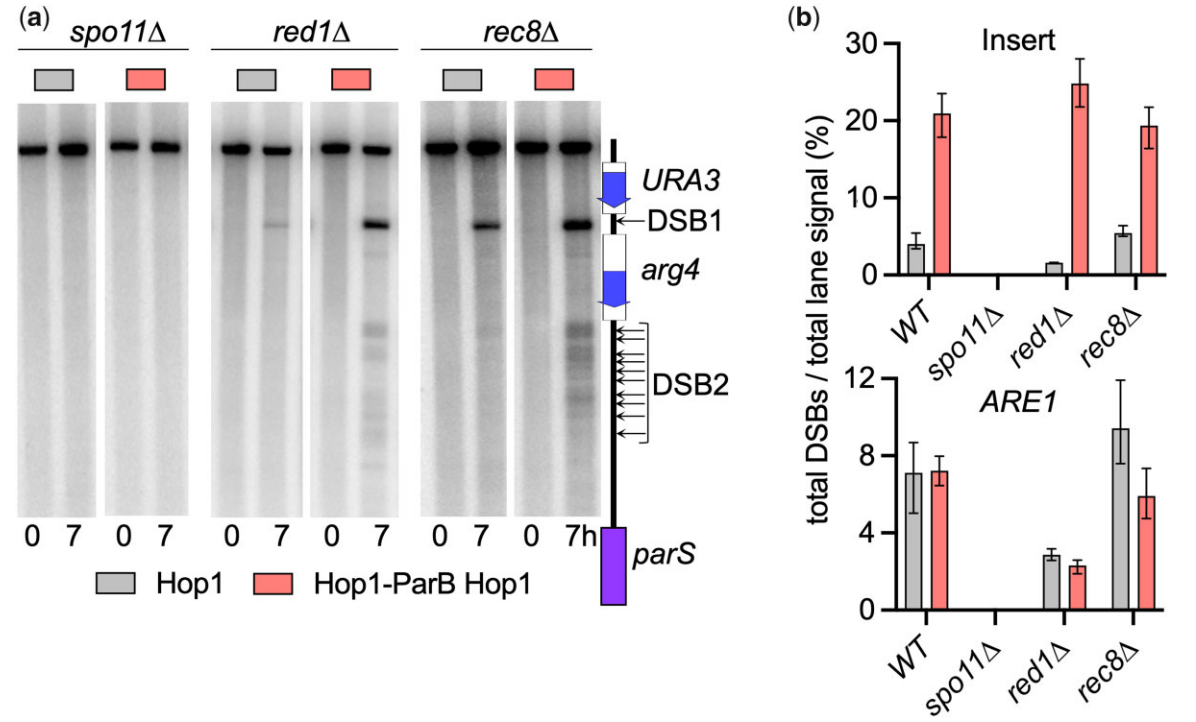

Fig. 4. Hop1-stimulated DSBs are Spo11 dependent but Red1- and Rec8-independent. a) Southern blot with DNA from a *sae2*Δ strain with inserts at *URA3* in *spo11*Δ, *red1*Δ or *rec8*Δ strains homozygous either for *HOP1* (gray) or *HOP1-parB HOP1* (salmon). DNA was digested with *Sbf*I and probed with *parS* sequences. b) Top—DSBs in the *parS* insert at *URA3*, measured at 7h after induction of meiosis in indicated mutant strains homozygous either for *HOP1* (gray) or *HOP1-parB HOP1* (salmon). Bottom—DSBs in the same strains at the *ARE1* control locus. Values in graphs are the average of 2 or more independent experiments; error bars denote range. See also Supplementary Fig. 3 and File 1, sheet 5.

heteroalleles inserted at *URA3* in these strains was reduced to about ∼40% of strains expressing both Hop1 and Hop1-ParB (*HOP1-parB HOP1/HOP1-parB HOP1*; Fig. 6b and Supplementary File 1, sheet 4), and DSBs at the *parS* insert locus and at the *ARE1* control locus were reduced to ∼45% and ∼18%, respectively (Fig. 6, c and d and Supplementary File 1, sheet 5), of DSB levels in strains expressing both Hop1 and Hop1-ParB (*HOP1-parB HOP1/HOP1-parB HOP1*). These defects were at least partially suppressed by the addition of a single copy of untagged *HOP1* (*HOP1-parB/HOP1*), while full suppression of the DSB defect required 2 wild-type copies of untagged *HOP1* (Fig. 6). Thus, while the Hop1-ParB fusion construct produces a protein that can recruit Hop1 protein to the region surrounding *parS*, it is unable to provide full Hop1 function.

Altered DSB repair in the presence of Hop1-ParB and in inserts at URA3

The Hop1-ParB fusion protein also conferred an apparent defect in meiotic DSB repair. Cells expressing Hop1-ParB showed a 45–50-min delay in the disappearance of DSBs both at the *parS* insert and at *ARE1* (Fig. 7, a, c, and d and Supplementary File 1, sheet 8). This delay was accompanied by a delay in meiotic divisions that increased with *HOP1-parB* gene dosage (Fig. 7b and Supplementary File 1, sheet 9), consistent with the presence of unrepaired DSBs activating the meiotic checkpoint (Lydall *et al.* 1996; Grushcow *et al.* 1999; Thompson and Stahl 1999; Roeder and Bailis 2000; Shimada *et al.* 2002).

In addition, Hop1-ParB-stimulated COs in inserts at *URA3* do not appear to use the CO recombination pathway that is dominant at other DSB hotspots. Previous studies indicate that most meiotic COs form via a pathway that involves the ZMM proteins and the meiosis-specific MutLγ resolvase (Mlh1-Mlh3-Exo1), and a minor fraction are formed by SSNs (Mus81-Mms4, Yen1, Slx1-Slx4; Schwacha and Kleckner 1994; Wang *et al.* 1999; Khazanehdari and Borts 2000; Kirkpatrick *et al.* 2000; Tsubouchi and Ogawa 2000; Allers and Lichten 2001a, 2001b; de los Santos *et al.* 2003; Hoffmann *et al.* 2003; Argueso *et al.* 2004; Bishop and Zickler 2004; Borner *et al.* 2004; Hollingsworth and Brill 2004; Jessop *et al.* 2006; Lynn *et al.* 2007; Jessop and Lichten 2008; Nishant *et al.* 2008; Zakharyevich *et al.* 2010; Comeron *et al.* 2012; De Muyt *et al.* 2012; Wang *et al.* 2012; Yang *et al.* 2012; Zakharyevich *et al.* 2012; Agostinho *et al.* 2013; Oke *et al.* 2014; Al-Sweel *et al.* 2017; De Muyt *et al.* 2018; Pyatnitskaya *et al.* 2019). However, genetic crossing-over in a ∼35-kb interval containing the *URA3-arg4*-pBR322-*parS* was reduced only modestly in *mlh3*Δ strains, both in strains where Hop1-ParB was expressed and where Hop1-parB was absent (Fig. 8 and Supplementary File 1, sheet 10).

We also measured CO and noncrossover (NCO) recombination at the molecular level, using a second *parS*-containing insert at *URA3* (*URA3-tel-ARG4-parB*; Fig. 9a) that contains a single DSB site (Jessop *et al.* 2005; Ahuja *et al.* 2021). Consistent with experiments described above that used *URA3-arg4*-pBR322-*parS* inserts, addition of a single copy of Hop1-ParB (*HOP1-parB HOP1/HOP1*) resulted in a marked increase in DSBs (∼7-fold; Fig. 9, a and b and Supplementary File 1, sheet 12), in COs (∼5-fold; Fig. 9, a, c, and d and Supplementary File 1, sheet 11), and in NCOs (∼4.5-fold; Supplementary Fig. 5, a and c and File 1, sheet 11) within the insert at *URA3*.

Previous studies have shown that *ndt80*Δ mutants arrest at the pachytene stage of meiosis with markedly reduced CO levels, regardless of whether MutLγ or SSNs are the primary resolvase (Xu *et al.* 1995; Chu and Herskowitz 1998; Allers and Lichten 2001a; Jessop and Lichten 2008; Sourirajan and Lichten 2008;

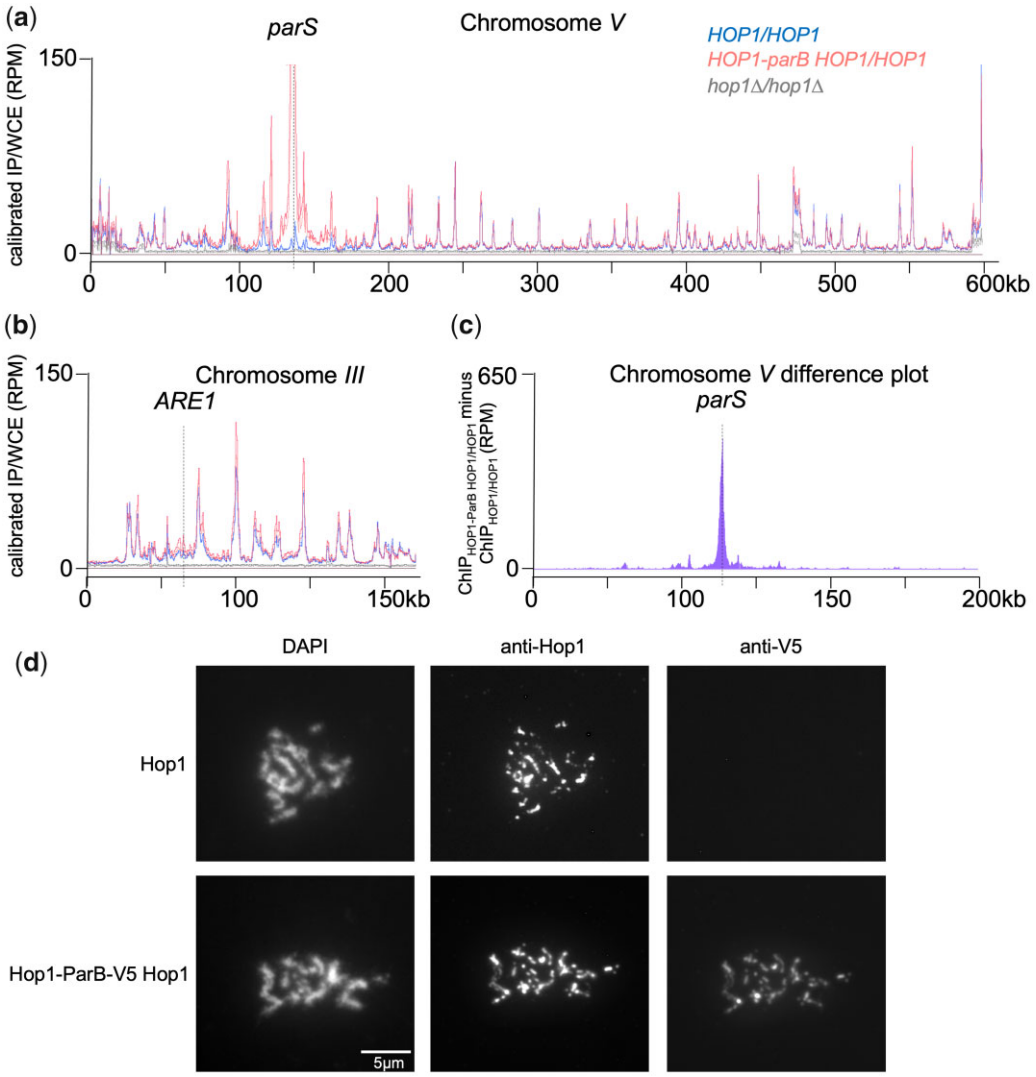

Fig. 5. Hop1 localization and enrichment at *parS*. a) Hop1 occupancy (immunoprecipitate [ChIP]/whole cell extract [WCE], reads per million) on chromosome V, determined by calibrated ChIP-seq (see *Materials and methods*) using samples taken at 4 h after induction of meiosis. Strains contained the *URA3-tel-arg4-parB* insert at *URA3* and the indicated *HOP1* genotype. Dark and light lines indicate replicates from independent experiments. Dotted vertical line—*parS* insert locus. The peak at *parS* in *HOP1-parB HOP1/HOP1* strains is truncated; peak values reached ∼700 RPM. b) Hop1 occupancy around the *ARE1* control locus (chr. *III*). Dotted vertical line—*ARE1* DSB site. All other details as in (a). c) Difference plot for 200 kb around *parS*, calculated by subtracting the calibrated ChIP/WCE for *HOP1/HOP1* (mean of both replicates) from that for *HOP1-parB HOP1/HOP1* (mean of both replicates). d) Chromosome spreads from meiotic cells (4 and 5 h postmeiotic induction) from wild type and from cells expressing Hop1-ParB (*HOP1-parB-V5 HOP1/HOP1*), probed with the indicated antiserum. In strains expressing Hop1-parB-V5, Hop1-ParB (anti-V5) shows the same distribution as total Hop1. Scale bar = 5μm. See also Supplementary Fig. 2.

De Muyt *et al.* 2012). Consistent with this, COs in the insert at *URA3* were reduced to about 1/3 to 1/4 of wild-type levels in *ndt80Δ* mutants, regardless of whether Hop1-ParB was present or absent (Fig. 9, c and d and Supplementary File 1, sheet 11). However, unlike at other hotspots, where *mlh3Δ* causes a ∼50% reduction in COs (Hunter and Borts 1997; Wang *et al.* 1999; Argueso *et al.* 2004; Nishant *et al.* 2008; Al-Sweel *et al.* 2017), *mlh3Δ* caused a much more modest 10–15% decrease in COs (Fig. 9, c and d and Supplementary File 1, sheet 11), as was seen in genetic crosses (Fig. 8b). Inactivation of the major mitotic resolvase Mus81-Mms4, in *mms4-md* mutants, reduced COs in inserts at *URA3* by 30–40% (Fig. 9, c and d and Supplementary File 1, sheet 11), as compared to reductions of 10–20% (*mus81* or *mms4*) seen at recombination hotspots (Borner *et al.* 2004; Jessop *et al.* 2006; Oh *et al.* 2007; De Muyt *et al.* 2012; Zakharyevich *et al.* 2012; He *et al.* 2020). COs were reduced by about 50% in *mlh3 mms4-md* double mutants, as compared to the ∼6-fold reduction reported in genetic studies (Argueso *et al.* 2004; Nishant *et al.* 2008; Brown *et al.* 2013). In these strains, COs were similarly affected whether Hop1-ParB was present or absent. Deletion of *YEN1* from *mlh3Δ mms4-md* strains did not further reduce COs when Hop1-ParB was present but caused a further reduction (to about 1/3 of wild type) in COs when only Hop1 was present (*mlh3Δ mms4-md yen1Δ*; Fig. 9, c and d and Supplementary File 1, sheet 11). Thus, regardless of DSB levels, the canonical, MutLγ-dependent pathway accounts for only a minor fraction of COs in inserts at *URA3*.

Discussion

The meiotic chromosome axis lies at the center of meiotic chromosome transactions, including the initiation of recombination by DSB formation, recombination partner choice and homolog

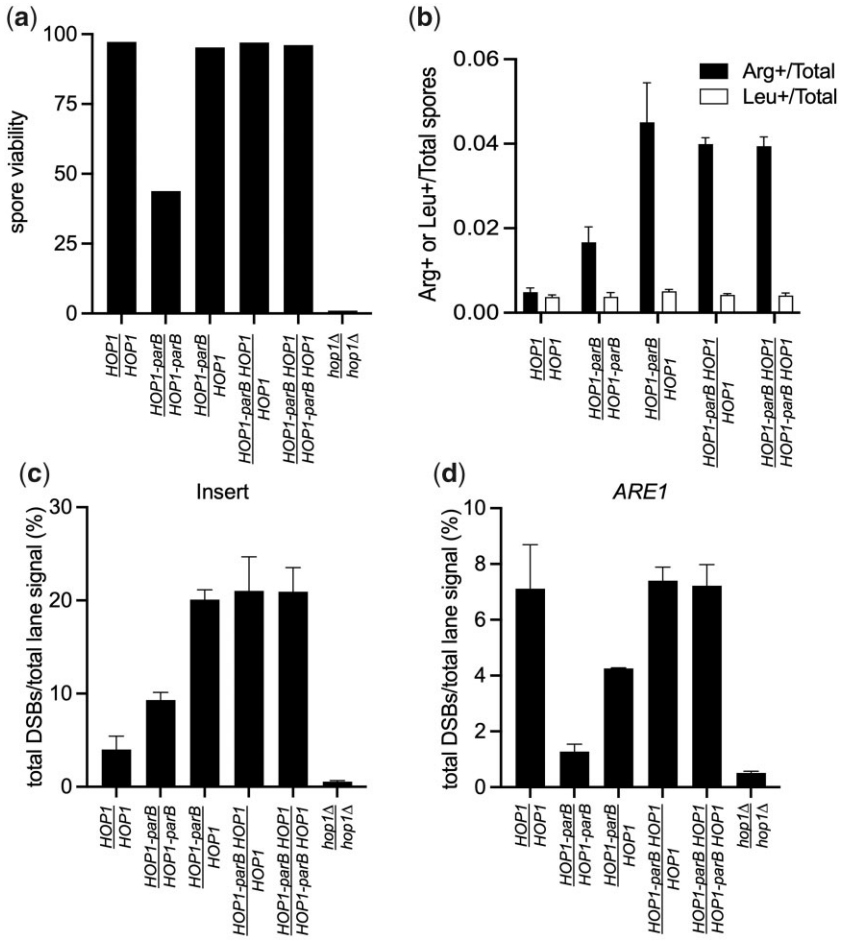

Fig. 6. Hop1-ParB has partial function. a) Spore viability in dissected tetrads. b) Frequencies of Arg+ (black) and Leu2+ (white) recombinants in random spores from diploids with the *URA3-ARG4-pBR322-parS* insert at *URA3*. c and d) Frequencies of DSBs (DSB1 + DSB2, see Fig. 3) at the *URA3-ARG4-pBR322-parS* insert at *URA3* and at the *ARE1* control locus, in *sae2*Δ strains. With the exception of panel (a), values in graphs are the average of 2 or more independent experiments; error bars denote range. See also Supplementary Fig. 3 and File 1, sheets 4, 5, and 7.

pairing, CO designation and pathway choice, and CO assurance and spacing control (Hollingsworth and Ponte 1997; Zickler and Kleckner 1999; Blat *et al.* 2002; Glynn *et al.* 2004; Kleckner 2006; Tsubouchi and Roeder 2006; Niu *et al.* 2007; Yang *et al.* 2008; Joshi *et al.* 2009; Kugou *et al.* 2009; Niu *et al.* 2009; Callender and Hollingsworth 2010; Kim *et al.* 2010; Panizza *et al.* 2011; Youds and Boulton 2011; Chuang *et al.* 2012; De Muyt *et al.* 2018; Pyatnitskaya *et al.* 2019; Ur and Corbett 2021; Hyppa *et al.* 2022). While axis proteins' roles in these processes have been extensively studied, the codependent localization of axis proteins has presented a challenge to the identification of their individual roles in meiotic recombination. In this article, we used the bacterial ParB-*parS* system to independently enrich the axis protein Hop1 at target loci, and to identify a unique role for Hop1 in DSB formation.

Hop1 is efficiently recruited by the ParB-parS system

While the ParB-*parS* system has previously been used as an alternative to operator-repressor arrays to visually label specific loci (Saad *et al.* 2014; Germier *et al.* 2018), the use of this system to recruit meiotic axis proteins is, to our knowledge, the first time that it has been used to localize chromosomal proteins with the goal of understanding their function. Hop1-ParB expression caused a markedly greater increase in Hop1 ChIP signal at the *parS* site and for about 25 kb to either side of *parS*, consistent with the spread of ParB from *parS* observed in bacteria, which is facilitated by its ability to dimerize and form a clamp that slides along DNA (Walter *et al.* 2020) and by its ability to bridge DNA (Breier and Grossman 2007; Graham *et al.* 2014; Antar *et al.* 2021).

Cytological analysis showed that Hop1-ParB and the wild-type Hop1 protein show similar nucleus-wide localization patterns (Fig. 5d), suggesting that the C-terminal tag does not prevent Hop1-ParB loading via Hop1-Red1 or Hop1-Hop1 interactions (West *et al.* 2018, 2019).

Hop1 determines local DSB levels

Previous studies have reported a direct correlation between levels of Hop1 (and Red1) enrichment and levels of Spo11 DSBs in different regions of the genome (Pan *et al.* 2011; Panizza *et al.* 2011; Subramanian *et al.* 2019). Here, we have shown that ParB-*parS*-mediated recruitment of Hop1 to a locus causes a dramatic increase in Spo11-dependent DSBs at that locus. This increase in DSBs is independent of the other meiosis-specific axis proteins, Red1 and Rec8. Thus, while Red1 and Rec8 might be required for Hop1 loading under normal circumstances, it is the level of Hop1 enrichment that ultimately determines the local DSB levels. This suggests that Hop1 alone is sufficient to recruit the DSB-forming Spo11 complex, consistent with recent biochemical studies

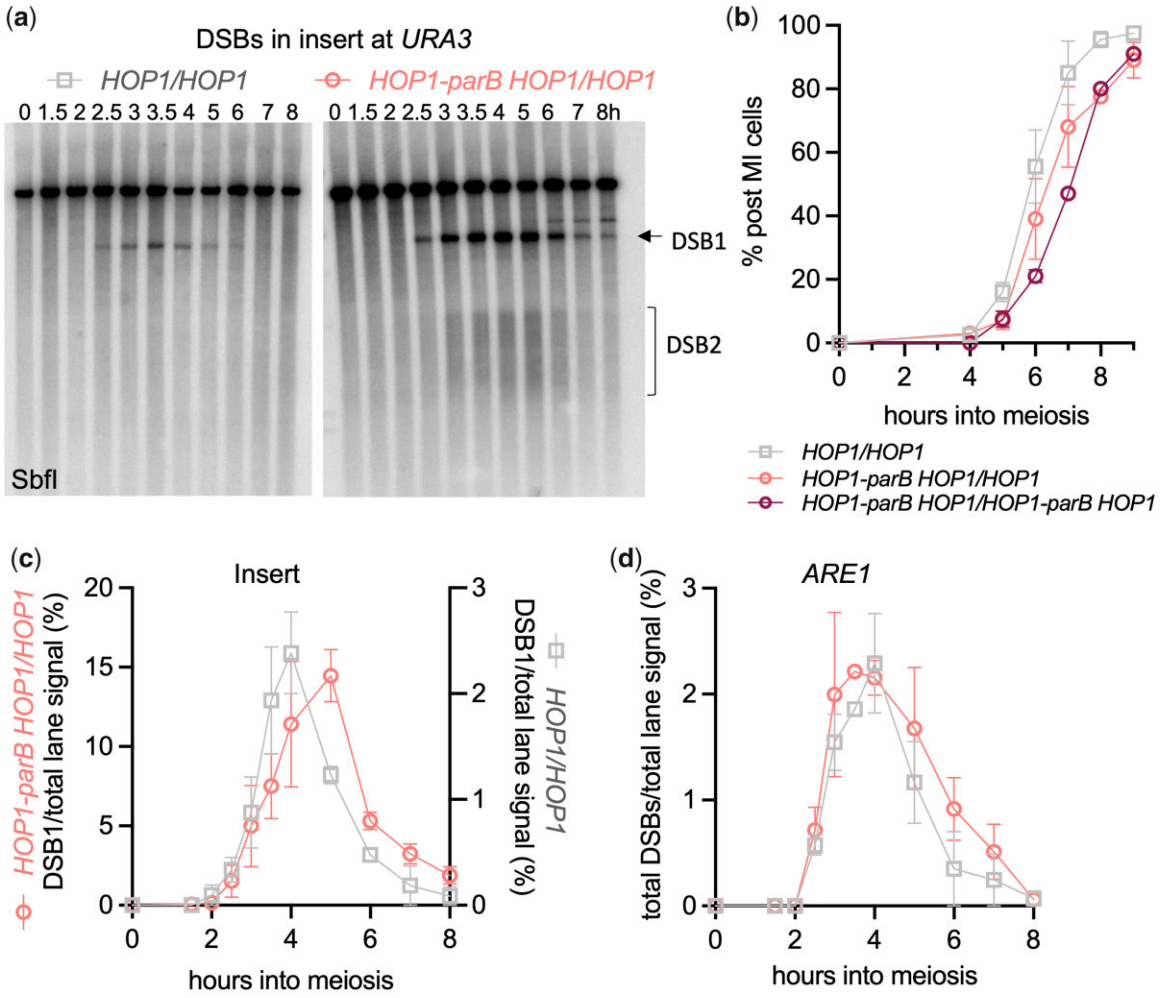

Fig. 7. Delayed DSB repair and meiotic progression in presence of Hop1-ParB. a) Southern blots of meiotic DNA from SAE2 cells with the *URA3-ARG4-pBR322-parS* insert at *URA3*, expressing either Hop1 or both Hop1-ParB and Hop1 digested with *Sbf1* and probed with *parS* sequences. The late-arising band above DSB1 is of the size expected for ectopic crossing-over or gene conversion between *URA3* sequences flanking the insert that removes a Ty1 insert in the left-hand copy of *URA3*. b) Meiotic progression, expressed as cells completing meiosis I (with either 2 or 4 nuclei). c) Quantification of total DSBs from the experiment in panel (a) and others. Note that data from strains expressing Hop1 (gray) are plotted with the right-hand Y axis, and from strains with *HOP1-ParB HOP1/HOP1* (salmon) on the left-hand Y axis with a different scale, to highlight DSB timing differences. d) DSBs at the *ARE1* control locus from the same experiments as in (c). Values in graphs are the average of 2 or more independent experiments; error bars denote range. See also Supplementary Fig. 4 and File 1, sheets 8 and 9.

showing that the Spo11 complex protein Mer2 interacts directly with Hop1 and not with Red1 (Rousová *et al.* 2021).

We found that, while Hop1-ParB can stimulate DSB formation in the vicinity of *par*S, Hop1-ParB alone was insufficient for optimal DSB formation, recombination, and spore viability, and that full function required addition of 1 to 2 copies of wild-type *HOP1*, depending upon the assay (Fig. 6). Since Hop1-ParB is produced at about 80–90% of the levels of wild-type Hop1 protein (Fig. 1b), it is unlikely that these results can be explained by reduced levels of Hop1 protein alone, although it is possible that over-enrichment of Hop1 at *par*S reduces Hop1 levels elsewhere in the genome. It also is possible that the presence of the C-terminal ParB tag creates a partially functional Hop1 protein. For example, recent *in vitro* studies have shown Mer2 preferentially binds to Hop1 with an unlocked closure motif (Rousová *et al.* 2021). Chromosome-bound Hop1 normally is in this unlocked configuration, due to closure motif-HORMA domain interactions that recruit it to the axis (West *et al.* 2018, 2019). However, Hop1 recruited to chromosomes by a ParB tag might frequently exist in the locked confirmation, and thus might recruit the Spo11 complex less efficiently. In addition, the ParB tag might interfere with interactions necessary for Hop1 posttranslational modification, and/or Hop1 loading/unloading (Carballo *et al.* 2008; Wojtasz *et al.* 2009; Thacker *et al.* 2014; Herruzo *et al.* 2016, 2021; Li and Shinohara 2021). For example, Hop1 is normally removed from the axis after homolog synapsis (Borner *et al.* 2008; Joshi *et al.* 2009; Wojtasz *et al.* 2009; Zanders and Alani 2009; Daniel *et al.* 2011; Kauppi *et al.* 2013; Thacker *et al.* 2014; Lambing *et al.* 2015; Subramanian *et al.* 2016, 2019); a failure to remove Hop1-ParB bound via the ParB tag might result in the persistent DSBs and delayed progression that we observed when Hop1-ParB is present (Fig. 7).

Noncanonical recombination pathway usage in inserts at the URA3 locus

Previous studies of CO formation have concluded that most meiotic COs are formed by MutLγ-dependent double Holliday junction resolution, a minor fraction are formed by mitotic resolvases (Mus81-Mms4/Eme1, Yen1/Gen1, and Slx1-Slx4) and that both modes of resolution are *CDC5*- and *NDT80*-dependent (Xu *et al.*

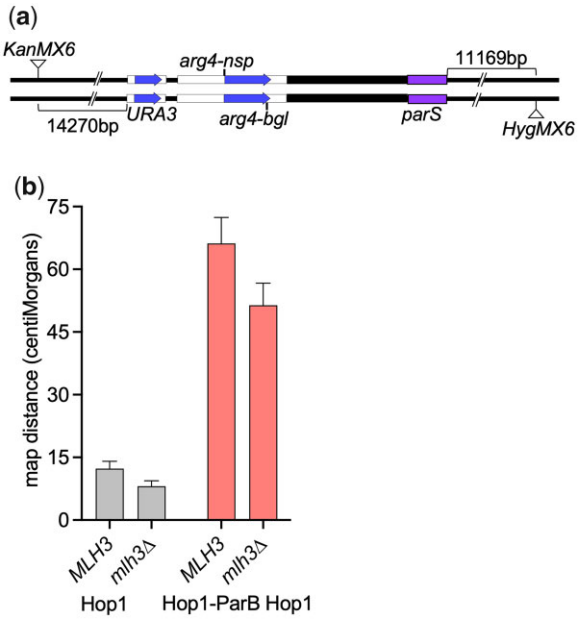

Fig. 8. Effect of *mlh3*Δ on CO at *URA3*. a) Schematic of the interval used to measure map distances by tetrad dissection. b) Map distances, calculated from marker segregation in tetrads, between *kanMX* and *hygMX* inserts flanking a *URA3-ARG4-pBR322-parS* insert at the *URA3* locus (shown in [a]; also see *Materials and methods*). Gray—*HOP1/HOP1*; salmon—*HOP1-parB HOP1/HOP1-parB HOP1*. Expression of Hop1-ParB results in a marked increase in map distances. Map distances are only modestly decreased in *mlh3*Δ strains. Error bars denote calculated standard error. See also Supplementary File 1, sheet 10.

1995; Chu and Herskowitz 1998; Allers and Lichten 2001a; Clyne *et al.* 2003; Jessop and Lichten 2008; Sourirajan and Lichten 2008; De Muyt *et al.* 2012; Schwartz *et al.* 2012; Zakharyevich *et al.* 2012; Blanco and Matos 2015; Yoon *et al.* 2016). These studies either examined events at recombination hotspots or examined crossing-over in large genetic intervals, in which presumably most recombination is hotspot driven. We find that recombination in inserts at *URA3* does not conform to these conclusions. While *ndt80*Δ substantially reduced COs (Fig. 9, c and d), consistent with crossing over in inserts at *URA3* being resolvase driven, specific resolvase dependence of COs was substantially altered. Unlike in previous studies, where loss of MutLγ results in a CO reduction by a factor of 2 (Hunter and Borts 1997; Wang *et al.* 1999; Argueso *et al.* 2004; Nishant *et al.* 2008; Al-Sweel *et al.* 2017), *mlh3*Δ mutants showed a substantially lower CO reduction (∼20–25% when measured genetically, Fig. 8b; ∼10–15% at the molecular level, Fig. 9, c and d). In addition, *mms4-md* mutants, which cause a meiosis-specific loss of Mus81-Mms4 activity, showed a substantial (30–40%) CO reduction in inserts at *URA3*, which is greater than the minor CO reductions seen in the absence of Mus81-Mms4 in other studies (Argueso *et al.* 2004; Jessop and Lichten 2008; De Muyt *et al.* 2012; Zakharyevich *et al.* 2012). Taken together, these data indicate a shift away from resolution by MutLγ, and toward resolution by mitotic resolvases during Spo11-induced recombination at *URA3*. Of particular importance, similar MutLγ-independence was seen in *HOP1/HOP1* and *HOP1-parB HOP1/HOP1* strains, even though DSB levels and CO levels differ more than 5-fold between these strains (Fig. 9). Intriguingly, when all 3 major resolvase activities were absent

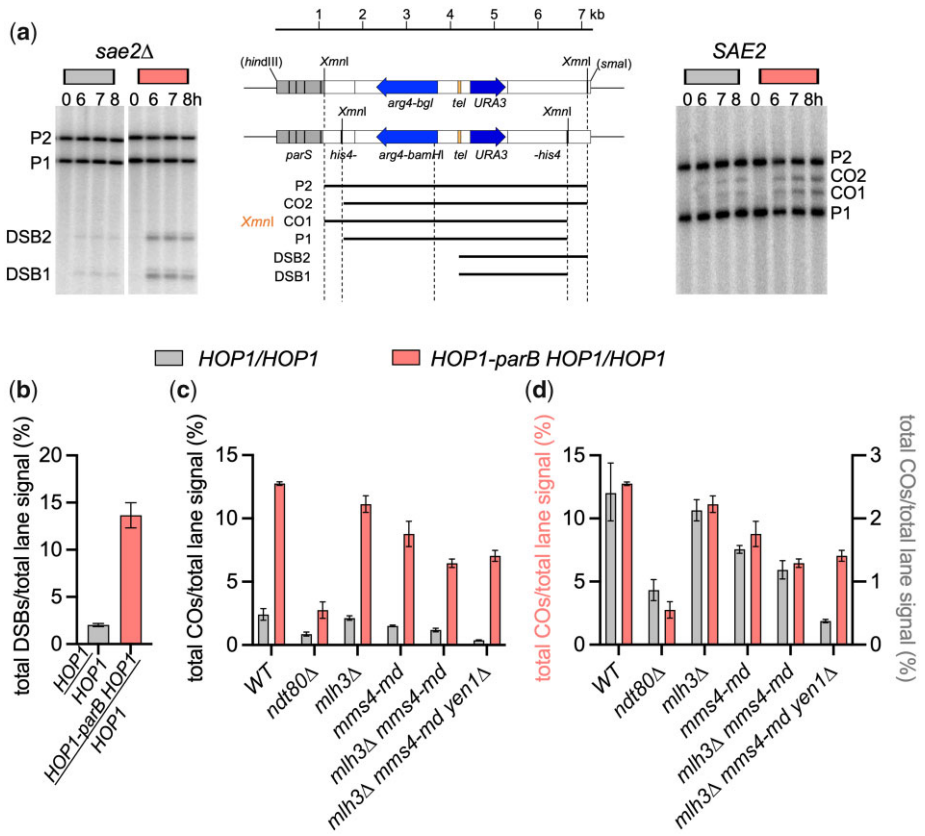

Fig. 9. Noncanonical CO pathway usage at *URA3*. a) Schematic for the *URA3-tel-arg4-parS* reporter insert at URA3, showing product lengths in *XmnI* digests. Left—Southern blots showing DSBs in *sae2*Δ strains; right—CO (CO1 and CO2) products in SAE2 strains. Both blots were probed with *URA3* sequences. b) Quantification of insert DSBs in *sae2*Δ *HOP1/HOP1* (gray) or *sae2*Δ *HOP1-parB HOP1/HOP1* (salmon) strains in samples taken 7h after meiotic induction. c) Quantification of COs (CO1 + CO2) in *HOP1/HOP1* (gray) or *HOP1-ParB HOP1/HOP1* (salmon) in samples taken 8 h after meiotic induction in the indicated mutants. d) Quantification of COs (CO1 + CO2) with a different scale for *HOP1/HOP1* (gray, right Y axis) and *HOP1-ParB HOP1/HOP1* (salmon, left Y axis) to compare relative levels in indicated mutants in the presence or absence of Hop1-ParB. Details as in panel (c). Values in graphs are the average of 2 or more independent experiments; error bars denote range. See also Supplementary Fig. 5 and File 1, sheets 11 and 12.

(*mlh3*Δ *mms4-md yen1*Δ), COs were markedly reduced when only Hop1 was present (to 15% of wild-type levels) but were still present at substantial levels (55% of wild type) when Hop1-ParB was present (Fig. 9, c and d and Supplementary File 1, sheet 11). This raises the possibility that either additional resolvases (such as Slx1-Slx4) or other repair pathways (such as break-induced replication) may be operating at loci with high DSB levels due to artificial Hop1 recruitment, as has been suggested for recombination in cells undergoing meiosis that is initiated by the VDE or HO site-specific nucleases (Medhi *et al.* 2016; Yisehak and MacQueen 2018; Shodhan *et al.* 2019).

One possible explanation for this is that Hop1-independent features of chromosome structure determine CO pathway choice. One such feature could be the axis proteins themselves. Red1 interacts with Zip4, a part of the ZZS complex and the larger ensemble of ZMM proteins that are important for the MutLγ-dependent CO pathway, and this interaction is conserved in other organisms (Yang *et al.* 2008; De Muyt *et al.* 2018; Pyatnitskaya *et al.* 2019). The meiotic cohesin component Rec8 has also been identified as playing a role in homolog bias and CO formation (Yoon *et al.* 2016; Hong *et al.* 2019), although this may simply reflect its role in recruiting Red1. If recruiting Hop1 to 'cold' regions increases DSB formation without increasing meiotic cohesin and/or Red1 levels, it is possible that insufficient ZMM proteins are recruited to promote MutLγ-dependent intermediate resolution, leading to an increased use of mitotic resolvases and of other pathways for CO formation.

In summary, we report here a novel use of the ParB-*parS* bacterial partition system, to study the role of chromosome structural proteins in meiotic recombination at a specific locus without substantially altering recombination elsewhere in the genome. The artificial recruitment of Hop1 to regions where meiotic axis proteins are normally low enabled the conversion of DSB/recombination coldspots into recombination hotspots by specifically increasing DSB formation independent of other axis proteins. Our data suggest an independent role for Hop1 in DSB formation, but also a need for the other axis proteins or other factors in normal repair pathway choice. It will be of interest to determine if recruiting both Red1 and Hop1 to these coldspots-turned hotspots can restore a more wild-type pattern of resolvase usage during meiotic CO formation. We also anticipate that artificial Hop1 recruitment could facilitate analysis of the interactions between Hop1 and Spo11 complex proteins that promote DSB formation. In addition, artificial recruitment of Hop1 homologs in other organism may provide a targeted way to increase meiotic recombination in regions where recombination is normally low, both for mechanistic studies and for breeding purposes.

Data availability

All strains and plasmids are available upon request. The authors affirm that all data necessary to confirm the conclusions of this article are represented within the article, tables, figures, supplementary materials, and publicly available database depositions. Supplemental files are available at figshare: https://doi.org/10.25386/genetics.20184515. Supplementary File 1 contains strain genotypes, primer and probe sequences, and numerical data underlying all graphs. Supplementary File 2 contains scripts implementing calibrated ChIP as a Snakemake workflow. Supplementary File 3 contains the sequence of plasmid pMJ1088. ChIP sequence reads are available at GEO, accession GSE201240.

Acknowledgments

We thank Darpan Medhi for suggesting the use of ParB-*parS* to recruit axis protein, Jasvinder Ahuja, Matan Cohen, Julie Cooper, Kevin Corbett, Yolanda L. Jones, Alex Kelly, and Hajime Murakami for helpful discussions and comments on the manuscript, Kevin Corbett for the gift of Hop1 protein used for antisera, and the Center for Cancer Research Genomics Core for high-throughput sequencing. This work used resources at the NIH HPC Biowulf cluster (https://hpc.nih.gov).

Funding

This work was supported by the Intramural Research Program of the NIH through the Center for Cancer Research at the National Cancer Institute. The funders had no role in research design, execution, analysis, interpretation, or reporting.

Conflicts of interest

None declared.

Literature cited

Acquaviva L, Székvölgyi L, Dichtl B, Dichtl BS, de La Roche Saint André C, Nicolas A, Géli V. The COMPASS subunit Spp1 links histone methylation to initiation of meiotic recombination. Science. 2013;339(6116):215–218.

Agostinho A, Meier B, Sonneville R, Jagut M, Woglar A, Blow J, Jantsch V, Gartner A. Combinatorial regulation of meiotic Holliday junction resolution in *C. elegans* by HIM-6 (BLM) helicase, SLX-4, and the SLX-1, MUS-81 and XPF-1 nucleases. PLoS Genet. 2013;9(7):e1003591.

Ahuja JS, Harvey CS, Wheeler DL, Lichten M. Repeated strand invasion and extensive branch migration are hallmarks of meiotic recombination. Mol Cell. 2021;81(20):4258–4270.e4254.

Al-Sweel N, Raghavan V, Dutta A, Ajith VP, Di Vietro L, Khondakar N, Manhart CM, Surtees JA, Nishant KT, Alani E, *et al. mlh3* mutations in baker's yeast alter meiotic recombination outcomes by increasing noncrossover events genome-wide. PLoS Genet. 2017;13(8):e1006974.

Allers T, Lichten M. A method for preparing genomic DNA that restrains branch migration of Holliday junctions. Nucleic Acids Res. 2000;28(2):e6.

Allers T, Lichten M. Differential timing and control of noncrossover and crossover recombination during meiosis. Cell. 2001a;106(1):47–57.

Allers T, Lichten M. Intermediates of yeast meiotic recombination contain heteroduplex DNA. Mol Cell. 2001b;8(1):225–231.

Antar H, Soh Y-M, Zamuner S, Bock FP, Anchimiuk A, Rios PDL, Gruber S. Relief of ParB autoinhibition by *parS* DNA catalysis and recycling of ParB by CTP hydrolysis promote bacterial centromere assembly. Sci Adv. 2021;7(41):eabj2854.

Argueso JL, Wanat J, Gemici Z, Alani E. Competing crossover pathways act during meiosis in *Saccharomyces cerevisiae*. Genetics. 2004;168(4):1805–1816.

Arora C, Kee K, Maleki S, Keeney S. Antiviral protein Ski8 is a direct partner of Spo11 in meiotic DNA break formation, independent of its cytoplasmic role in RNA metabolism. Mol Cell. 2004;13(4):549–559.

Attaiech L, Minnen A, Kjos M, Gruber S, Veening JW. The ParB-*parS* chromosome segregation system modulates competence development in *Streptococcus pneumoniae*. MBio. 2015;6(4):e00662.

Baudat F, de Massy B. Regulating double-stranded DNA break repair towards crossover or non-crossover during mammalian meiosis. Chromosome Res. 2007;15(5):565–577.

Berezney R, Dubey DD, Huberman JA. Heterogeneity of eukaryotic replicons, replicon clusters, and replication foci. Chromosoma. 2000;108(8):471–484.

Bergerat A, de Massy B, Gadelle D, Varoutas PC, Nicolas A, Forterre P. An atypical topoisomerase II from *Archaea* with implications for meiotic recombination. Nature. 1997;386(6623):414–417.

Bishop DK, Zickler D. Early decision; meiotic crossover interference prior to stable strand exchange and synapsis. Cell. 2004;117(1):9–15.

Blanco MG, Matos J. Hold your horSSEs: controlling structure-selective endonucleases MUS81 and Yen1/GEN1. Front Genet. 2015;6:253.

Blat Y, Protacio RU, Hunter N, Kleckner N. Physical and functional interactions among basic chromosome organizational features govern early steps of meiotic chiasma formation. Cell. 2002;111(6):791–802.

Borde V, Wu TC, Lichten M. Use of a recombination reporter insert to define meiotic recombination domains on chromosome *III* of *Saccharomyces cerevisiae*. Mol Cell Biol. 1999;19(7):4832–4842.

Borner GV, Barot A, Kleckner N. Yeast Pch2 promotes domainal axis organization, timely recombination progression, and arrest of defective recombinosomes during meiosis. Proc Natl Acad Sci USA. 2008;105(9):3327–3332.

Borner GV, Kleckner N, Hunter N. Crossover/noncrossover differentiation, synaptonemal complex formation, and regulatory surveillance at the leptotene/zygotene transition of meiosis. Cell. 2004;117(1):29–45.

Breier AM, Grossman AD. Whole-genome analysis of the chromosome partitioning and sporulation protein Spo0J (ParB) reveals spreading and origin-distal sites on the *Bacillus subtilis* chromosome. Mol Microbiol. 2007;64(3):703–718.

Brown MS, Lim E, Chen C, Nishant KT, Alani E. Genetic analysis of *mlh3* mutations reveals interactions between crossover promoting factors during meiosis in baker's yeast. G3 (Bethesda). 2013;3(1):9–22.

Callender TL, Hollingsworth NM. Mek1 suppression of meiotic double-strand break repair is specific to sister chromatids, chromosome autonomous and independent of Rec8 cohesin complexes. Genetics. 2010;185(3):771–782.

Cannavo E, Sanchez A, Anand R, Ranjha L, Hugener J, Adam C, Acharya A, Weyland N, Aran-Guiu X, Charbonnier J-B, *et al.* Regulation of the MLH1-MLH3 endonuclease in meiosis. Nature. 2020;586(7830):618–622.

Carballo JA, Johnson AL, Sedgwick SG, Cha RS. Phosphorylation of the axial element protein Hop1 by Mec1/Tel1 ensures meiotic interhomolog recombination. Cell. 2008;132(5):758–770.

Caryl AP, Armstrong SJ, Jones GH, Franklin FC. A homologue of the yeast HOP1 gene is inactivated in the *Arabidopsis* meiotic mutant *asy1*. Chromosoma. 2000;109(1–2):62–71.

Chen S, Zhou Y, Chen Y, Gu J. fastp: an ultra-fast all-in-one FASTQ preprocessor. Bioinformatics. 2018;34(17):i884–i890.

Chu S, Herskowitz I. Gametogenesis in yeast is regulated by a transcriptional cascade dependent on Ndt80. Mol Cell. 1998;1(5):685–696.

Chuang CN, Cheng YH, Wang TF. Mek1 stabilizes Hop1-Thr318 phosphorylation to promote interhomolog recombination and checkpoint responses during yeast meiosis. Nucleic Acids Res. 2012;40(22):11416–11427.

Claeys Bouuaert C, Pu S, Wang J, Oger C, Daccache D, Xie W, Patel DJ, Keeney S. DNA-driven condensation assembles the meiotic DNA break machinery. Nature. 2021;592(7852):144–149.

Clyne RK, Katis VL, Jessop L, Benjamin KR, Herskowitz I, Lichten M, Nasmyth K. Polo-like kinase Cdc5 promotes chiasmata formation and cosegregation of sister centromeres at meiosis I. Nat Cell Biol. 2003;5(5):480–485.

Comeron JM, Ratnappan R, Bailin S. The many landscapes of recombination in *Drosophila melanogaster*. PLoS Genet. 2012;8(10):e1002905.

Daniel K, Lange J, Hached K, Fu J, Anastassiadis K, Roig I, Cooke HJ, Stewart AF, Wassmann K, Jasin M, *et al.* Meiotic homologue alignment and its quality surveillance are controlled by mouse HORMAD1. Nat Cell Biol. 2011;13(5):599–610.

Davidson IF, Bauer B, Goetz D, Tang W, Wutz G, Peters J-M. DNA loop extrusion by human cohesin. Science. 2019;366(6471):1338–1345.

de los Santos T, Hollingsworth NM. Red1p, a *MEK1*-dependent phosphoprotein that physically interacts with Hop1p during meiosis in yeast. J Biol Chem. 1999;274(3):1783–1790.

de los Santos T, Hunter N, Lee C, Larkin B, Loidl J, Hollingsworth NM. The Mus81/Mms4 endonuclease acts independently of double-Holliday junction resolution to promote a distinct subset of crossovers during meiosis in budding yeast. Genetics. 2003;164(1):81–94.

De Muyt A, Jessop L, Kolar E, Sourirajan A, Chen J, Dayani Y, Lichten M. BLM helicase ortholog Sgs1 is a central regulator of meiotic recombination intermediate metabolism. Mol Cell. 2012;46(1):43–53.

De Muyt A, Pyatnitskaya A, Andréani J, Ranjha L, Ramus C, Laureau R, Fernandez-Vega A, Holoch D, Girard E, Govin J, *et al.* A meiotic XPF-ERCC1-like complex recognizes joint molecule recombination intermediates to promote crossover formation. Genes Dev. 2018;32(3–4):283–296.

Dubarry N, Pasta F, Lane D. ParABS systems of the four replicons of *Burkholderia cenocepacia*: new chromosome centromeres confer partition specificity. J Bacteriol. 2006;188(4):1489–1496.

Dujon B. Yeasts illustrate the molecular mechanisms of eukaryotic genome evolution. Trends Genet. 2006;22(7):375–387.

Funakoshi M, Hochstrasser M. Small epitope-linker modules for PCR-based C-terminal tagging in *Saccharomyces cerevisiae*. Yeast. 2009;26(3):185–192.

Gao Y, Kardos J, Yang Y, Tamir TY, Mutter-Rottmayer E, Weissman B, Major MB, Kim WY, Vaziri C. The cancer/testes (CT) antigen HORMAD1 promotes homologous recombinational DNA repair and radioresistance in lung adenocarcinoma cells. Sci Rep. 2018;8(1):15304.

Germier T, Audibert S, Kocanova S, Lane D, Bystricky K. Real-time imaging of specific genomic loci in eukaryotic cells using the ANCHOR DNA labelling system. Methods. 2018;142:16–23.

Glynn EF, Megee PC, Yu H-G, Mistrot C, Unal E, Koshland DE, DeRisi JL, Gerton JL. Genome-wide mapping of the cohesin complex in the yeast *Saccharomyces cerevisiae*. PLoS Biol. 2004;2(9):E259.

Goldfarb T, Lichten M. Frequent and efficient use of the sister chromatid for DNA double-strand break repair during budding yeast meiosis. PLoS Biol. 2010;8(10):e1000520.

Goldway M, Sherman A, Zenvirth D, Arbel T, Simchen G. A short chromosomal region with major roles in yeast chromosome *III* meiotic disjunction, recombination and double strand breaks. Genetics. 1993;133(2):159–169.

Golfier S, Quail T, Kimura H, Brugues J. Cohesin and condensin extrude DNA loops in a cell cycle-dependent manner. Elife. 2020;9: e53885.

Goyon C, Lichten M. Timing of molecular events in meiosis in *Saccharomyces cerevisiae*: stable heteroduplex DNA is formed late in meiotic prophase. Mol Cell Biol. 1993;13(1):373–382.

Graham TGW, Wang X, Song D, Etson CM, van Oijen AM, Rudner DZ, Loparo JJ. ParB spreading requires DNA bridging. Genes Dev. 2014;28(11):1228–1238.

Grushcow JM, Holzen TM, Park KJ, Weinert T, Lichten M, Bishop DK. *Saccharomyces cerevisiae* checkpoint genes *MEC1, RAD17* and *RAD24* are required for normal meiotic recombination partner choice. Genetics. 1999;153(2):607–620.

Hadjur S, Williams LM, Ryan NK, Cobb BS, Sexton T, Fraser P, Fisher AG, Merkenschlager M. Cohesins form chromosomal cis-interactions at the developmentally regulated IFNG locus. Nature. 2009;460(7253):410–413.

Hassold T, Hunt P. To err (meiotically) is human: the genesis of human aneuploidy. Nat Rev Genet. 2001;2(4):280–291.

He W, Rao HBDP, Tang S, Bhagwat N, Kulkarni DS, Ma Y, Chang MAW, Hall C, Bragg JW, Manasca HS, *et al.* Regulated proteolysis of MutSgamma controls meiotic crossing over. Mol Cell. 2020; 78(1):168–183.e165.

Heldrich J, Markowitz TE, Vale-Silva LA, Hochwagen A. A cohesin-independent mechanism modulates recombination activity along meiotic chromosomes. bioRxiv 2020.08.11.247122. 2020. https://doi.org/10.1101/2020.08.11.247122.

Heldrich J, Milano CR, Markowitz TE, Ur SN, Vale-Silva LA, Corbett KD, Hochwagen A. Two pathways drive meiotic chromosome axis assembly in Saccharomyces cerevisiae. Nucleic Acids Res. 2022;50(8):4545–4556.

Henderson KA, Kee K, Maleki S, Santini PA, Keeney S. Cyclin-dependent kinase directly regulates initiation of meiotic recombination. Cell. 2006;125(7):1321–1332.

Herruzo E, Lago-Maciel A, Baztán S, Santos B, Carballo JA, San-Segundo PA. Pch2 orchestrates the meiotic recombination checkpoint from the cytoplasm. PLoS Genet. 2021;17(7):e1009560.

Herruzo E, Ontoso D, González-Arranz S, Cavero S, Lechuga A, San-Segundo PA. The Pch2 AAA+ ATPase promotes phosphorylation of the Hop1 meiotic checkpoint adaptor in response to synaptonemal complex defects. Nucleic Acids Res. 2016;44(16): 7722–7741.

Hoffmann ER, Shcherbakova PV, Kunkel TA, Borts RH. *MLH1* mutations differentially affect meiotic functions in *Saccharomyces cerevisiae*. Genetics. 2003;163(2):515–526.

Hollingsworth NM, Brill SJ. The Mus81 solution to resolution: generating meiotic crossovers without Holliday junctions. Genes Dev. 2004;18(2):117–125.

Hollingsworth NM, Byers B. *HOP1*: a yeast meiotic pairing gene. Genetics. 1989;121(3):445–462.

Hollingsworth NM, Ponte L. Genetic interactions between *HOP1*, *RED1* and *MEK1* suggest that *MEK1* regulates assembly of axial element components during meiosis in the yeast *Saccharomyces cerevisiae*. Genetics. 1997;147(1):33–42.

Hong S, Joo JH, Yun H, Kleckner N, Kim KP. Recruitment of Rec8, Pds5 and Rad61/Wapl to meiotic homolog pairing, recombination, axis formation and S-phase. Nucleic Acids Res. 2019;47(22): 11691–11708.

Hunter N, Borts RH. Mlh1 is unique among mismatch repair proteins in its ability to promote crossing-over during meiosis. Genes Dev. 1997;11(12):1573–1582.

Hyppa RW, Cho JD, Nambiar M, Smith GR. Redirecting meiotic DNA break hotspot determinant proteins alters localized spatial control of DNA break formation and repair. Nucleic Acids Res. 2022; 50(2):899–914.

Jessop L, Allers T, Lichten M. Infrequent co-conversion of markers flanking a meiotic recombination initiation site in *Saccharomyces cerevisiae*. Genetics. 2005;169(3):1353–1367.

Jessop L, Lichten M. Mus81/Mms4 endonuclease and Sgs1 helicase collaborate to ensure proper recombination intermediate metabolism during meiosis. Mol Cell. 2008;31(3):313–323.

Jessop L, Rockmill B, Roeder GS, Lichten M. Meiotic chromosome synapsis-promoting proteins antagonize the anti-crossover activity of Sgs1. PLoS Genet. 2006;2(9):e155.

Jin H, Guacci V, Yu HG. Pds5 is required for homologue pairing and inhibits synapsis of sister chromatids during yeast meiosis. J Cell Biol. 2009;186(5):713–725.

Joshi N, Barot A, Jamison C, Borner GV. Pch2 links chromosome axis remodeling at future crossover sites and crossover distribution during yeast meiosis. PLoS Genet. 2009;5(7):e1000557.

Kane SM, Roth R. Carbohydrate metabolism during ascospore development in yeast. J Bacteriol. 1974;118(1):8–14.

Kariyazono R, Oda A, Yamada T, Ohta K. Conserved HORMA domain-containing protein Hop1 stabilizes interaction between proteins of meiotic DNA break hotspots and chromosome axis. Nucleic Acids Res. 2019;47(19):10166–10180.

Katis VL, Lipp JJ, Imre R, Bogdanova A, Okaz E, Habermann B, Mechtler K, Nasmyth K, Zachariae W. Rec8 phosphorylation by casein kinase 1 and Cdc7-Dbf4 kinase regulates cohesin cleavage by separase during meiosis. Dev Cell. 2010;18(3):397–409.

Kauppi L, Barchi M, Lange J, Baudat F, Jasin M, Keeney S. Numerical constraints and feedback control of double-strand breaks in mouse meiosis. Genes Dev. 2013;27(8):873–886.

Kaur H, Ahuja JS, Lichten M. Methods for controlled protein depletion to study protein function during meiosis. Methods Enzymol. 2018;601:331–357.

Kee K, Keeney S. Functional interactions between *SPO11* and *REC102* during initiation of meiotic recombination in *Saccharomyces cerevisiae*. Genetics. 2002;160(1):111–122.

Kee K, Protacio RU, Arora C, Keeney S. Spatial organization and dynamics of the association of Rec102 and Rec104 with meiotic chromosomes. Embo J. 2004;23(8):1815–1824.

Keeney S. Mechanism and control of meiotic recombination initiation. Curr Top Dev Biol. 2001;52:1–53.

Keeney S, Kleckner N. Covalent protein-DNA complexes at the 5' strand termini of meiosis-specific double-strand breaks in yeast. Proc Natl Acad Sci USA. 1995;92(24):11274–11278.

Kellis M, Patterson N, Endrizzi M, Birren B, Lander ES. Sequencing and comparison of yeast species to identify genes and regulatory elements. Nature. 2003;423(6937):241–254.

Khare D, Ziegelin G, Lanka E, Heinemann U. Sequence-specific DNA binding determined by contacts outside the helix-turn-helix motif of the ParB homolog KorB. Nat Struct Mol Biol. 2004;11(7): 656–663.

Khazanehdari KA, Borts RH. *EXO1* and *MSH4* differentially affect crossing-over and segregation. Chromosoma. 2000;109(1–2): 94–102.

Kim KP, Weiner BM, Zhang L, Jordan A, Dekker J, Kleckner N. Sister cohesion and structural axis components mediate homolog bias of meiotic recombination. Cell. 2010;143(6):924–937.

Kim Y, Rosenberg SC, Kugel CL, Kostow N, Rog O, Davydov V, Su TY, Dernburg AF, Corbett KD. The chromosome axis controls meiotic events through a hierarchical assembly of HORMA domain proteins. Dev Cell. 2014;31(4):487–502.

Kim Y, Shi Z, Zhang H, Finkelstein IJ, Yu H. Human cohesin compacts DNA by loop extrusion. Science. 2019;366(6471):1345–1349.

Kirkpatrick DT, Ferguson JR, Petes TD, Symington LS. Decreased meiotic intergenic recombination and increased meiosis I nondisjunction in *exo1* mutants of *Saccharomyces cerevisiae*. Genetics. 2000;156(4):1549–1557.

Kironmai KM, Muniyappa K, Friedman DB, Hollingsworth NM, Byers B. DNA-binding activities of Hop1 protein, a synaptonemal complex component from *Saccharomyces cerevisiae*. Mol Cell Biol. 1998;18(3):1424–1435.

Kleckner N. Chiasma formation: chromatin/axis interplay and the role(s) of the synaptonemal complex. Chromosoma. 2006;115(3):175–194.

Klein F, Mahr P, Galova M, Buonomo SB, Michaelis C, Nairz K, Nasmyth K. A central role for cohesins in sister chromatid cohesion, formation of axial elements, and recombination during yeast meiosis. Cell. 1999;98(1):91–103.

Kshirsagar R, Khan K, Joshi MV, Hosur RV, Muniyappa K. Probing the potential role of non-B DNA structures at yeast meiosis-specific DNA double-strand breaks. Biophys J. 2017;112(10):2056–2074.

Kugou K, Fukuda T, Yamada S, Ito M, Sasanuma H, Mori S, Katou Y, Itoh T, Matsumoto K, Shibata T, *et al.* Rec8 guides canonical Spo11 distribution along yeast meiotic chromosomes. Mol Biol Cell. 2009;20(13):3064–3076.

Kulkarni DS, Owens SN, Honda M, Ito M, Yang Y, Corrigan MW, Chen L, Quan AL, Hunter N. PCNA activates the MutLg endonuclease to promote meiotic crossing over. Nature. 2020;586(7830):623–627.

Lam I, Keeney S. Nonparadoxical evolutionary stability of the recombination initiation landscape in yeast. Science. 2015;350(6263):932–937.

Lambing C, Osman K, Nuntasoontorn K, West A, Higgins JD, Copenhaver GP, Yang J, Armstrong SJ, Mechtler K, Roitinger E, *et al. Arabidopsis* PCH2 mediates meiotic chromosome remodeling and maturation of crossovers. PLoS Genet. 2015;11(7):e1005372.

Li H. Minimap2: pairwise alignment for nucleotide sequences. Bioinformatics. 2018;34(18):3094–3100.

Li J, Hooker GW, Roeder GS. *Saccharomyces cerevisiae* Mer2, Mei4 and Rec114 form a complex required for meiotic double-strand break formation. Genetics. 2006;173(4):1969–1981.

Li K, Shinohara M. Meiotic DSB-independent role of protein phosphatase 4 in Hop1 assembly to promote meiotic chromosome axis formation in budding yeast. bioRxiv 2021. https://doi.org/10.1101/2021.05.10.443451.

Lichten M, Borts RH, Haber JE. Meiotic gene conversion and crossing over between dispersed homologous sequences occurs frequently in *Saccharomyces cerevisiae*. Genetics. 1987;115(2):233–246.

Lin DC, Grossman AD. Identification and characterization of a bacterial chromosome partitioning site. Cell. 1998;92(5):675–685.

Liti G, Nguyen Ba AN, Blythe M, Müller CA, Bergström A, Cubillos FA, Dafhnis-Calas F, Khoshraftar S, Malla S, Mehta N, *et al.* High quality de novo sequencing and assembly of the *Saccharomyces arboricolus* genome. BMC Genomics. 2013;14:69.

Loidl J, Nairz K, Klein F. Meiotic chromosome synapsis in a haploid yeast. Chromosoma. 1991;100(4):221–228.

Lorenz A. New cassettes for single-step drug resistance and prototrophic marker switching in fission yeast. Yeast. 2015;32(12):703–710.

Lorenz A, Wells JL, Pryce DW, Novatchkova M, Eisenhaber F, McFarlane RJ, Loidl J. *S. pombe* meiotic linear elements contain proteins related to synaptonemal complex components. J Cell Sci. 2004;117(Pt 15):3343–3351.

Lydall D, Nikolsky Y, Bishop DK, Weinert T. A meiotic recombination checkpoint controlled by mitotic checkpoint genes. Nature. 1996;383(6603):840–843.

Lynn A, Soucek R, Borner GV. ZMM proteins during meiosis: crossover artists at work. Chromosome Res. 2007;15(5):591–605.

Makrantoni V, Robertson D, Marston AL. Analysis of the chromosomal localization of yeast SMC complexes by chromatin immunoprecipitation. Methods Mol Biol. 2019;2004:119–138.

Maleki S, Neale MJ, Arora C, Henderson KA, Keeney S. Interactions between Mei4, Rec114, and other proteins required for meiotic DNA double-strand break formation in *Saccharomyces cerevisiae*. Chromosoma. 2007;116(5):471–486.

Malone RE, Bullard S, Hermiston M, Rieger R, Cool M, Galbraith A. Isolation of mutants defective in early steps of meiotic recombination in the yeast *Saccharomyces cerevisiae*. Genetics. 1991;128(1):79–88.

Mao-Draayer Y, Galbraith AM, Pittman DL, Cool M, Malone RE. Analysis of meiotic recombination pathways in the yeast *Saccharomyces cerevisiae*. Genetics. 1996;144(1):71–86.

Martinez-Perez E, Villeneuve AM. HTP-1-dependent constraints coordinate homolog pairing and synapsis and promote chiasma formation during *C. elegans* meiosis. Genes Dev. 2005;19(22):2727–2743.

Matos J, Blanco MG, Maslen S, Skehel JM, West SC. Regulatory control of the resolution of DNA recombination intermediates during meiosis and mitosis. Cell. 2011;147(1):158–172.

Medhi D, Goldman AS, Lichten M. Local chromosome context is a major determinant of crossover pathway biochemistry during budding yeast meiosis. Elife. 2016;5:e19669.

Mölder F, Jablonski KP, Letcher B, Hall MB, Tomkins-Tinch CH, Sochat V, Forster J, Lee S, Twardziok SO, Kanitz A, *et al.* Sustainable data analysis with Snakemake. F1000Res. 2021;10:33.

Murakami H, Keeney S. Temporospatial coordination of meiotic DNA replication and recombination via DDK recruitment to replisomes. Cell. 2014;158(4):861–873.

Murray H, Ferreira H, Errington J. The bacterial chromosome segregation protein Spo0J spreads along DNA from *parS* nucleation sites. Mol Microbiol. 2006;61(5):1352–1361.

Nativio R, Wendt KS, Ito Y, Huddleston JE, Uribe-Lewis S, Woodfine K, Krueger C, Reik W, Peters J-M, Murrell A, *et al.* Cohesin is required for higher-order chromatin conformation at the imprinted IGF2-H19 locus. PLoS Genet. 2009;5(11):e1000739.

Nishant KT, Plys AJ, Alani E. A mutation in the putative *MLH3* endonuclease domain confers a defect in both mismatch repair and meiosis in *Saccharomyces cerevisiae*. Genetics. 2008;179(2):747–755.

Niu H, Li X, Job E, Park C, Moazed D, Gygi SP, Hollingsworth NM. Mek1 kinase is regulated to suppress double-strand break repair between sister chromatids during budding yeast meiosis. Mol Cell Biol. 2007;27(15):5456–5467.

Niu H, Wan L, Baumgartner B, Schaefer D, Loidl J, Hollingsworth NM. Partner choice during meiosis is regulated by Hop1-promoted dimerization of Mek1. Mol Biol Cell. 2005;16(12):5804–5818.

Niu H, Wan L, Busygina V, Kwon Y, Allen JA, Li X, Kunz RC, Kubota K, Wang B, Sung P, *et al.* Regulation of meiotic recombination via Mek1-mediated Rad54 phosphorylation. Mol Cell. 2009;36(3):393–404.

Nonomura K-I, Nakano M, Murata K, Miyoshi K, Eiguchi M, Miyao A, Hirochika H, Kurata N. An insertional mutation in the rice *PAIR2* gene, the ortholog of *Arabidopsis ASY1*, results in a defect in homologous chromosome pairing during meiosis. Mol Genet Genomics. 2004;271(2):121–129.

Oh SD, Lao JP, Hwang PY-H, Taylor AF, Smith GR, Hunter N. BLM ortholog, Sgs1, prevents aberrant crossing-over by suppressing formation of multichromatid joint molecules. Cell. 2007;130(2): 259–272.

Oke A, Anderson CM, Yam P, Fung JC. Controlling meiotic recombinational repair - specifying the roles of ZMMs, Sgs1 and Mus81/Mms4 in crossover formation. PLoS Genet. 2014;10(10):e1004690.

Pan J, Sasaki M, Kniewel R, Murakami H, Blitzblau HG, Tischfield SE, Zhu X, Neale MJ, Jasin M, Socci ND, *et al.* A hierarchical combination of factors shapes the genome-wide topography of yeast meiotic recombination initiation. Cell. 2011;144(5):719–731.

Panizza S, Mendoza MA, Berlinger M, Huang L, Nicolas A, Shirahige K, Klein F. Spo11-accessory proteins link double-strand break sites to the chromosome axis in early meiotic recombination. Cell. 2011;146(3):372–383.

Peciña A, Smith KN, Mézard C, Murakami H, Ohta K, Nicolas A. Targeted stimulation of meiotic recombination. Cell. 2002;111(2): 173–184.

Perkins DD. Biochemical mutants in the smut fungus *Ustilago maydis*. Genetics. 1949;34(5):607–626.

Prieler S, Penkner A, Borde V, Klein F. The control of Spo11's interaction with meiotic recombination hotspots. Genes Dev. 2005;19(2): 255–269.

Prinz S, Amon A, Klein F. Isolation of *COM1*, a new gene required to complete meiotic double-strand break-induced recombination in *Saccharomyces cerevisiae*. Genetics. 1997;146(3):781–795.

Pyatnitskaya A, Borde V, De Muyt A. Crossing and zipping: molecular duties of the ZMM proteins in meiosis. Chromosoma. 2019;128(3): 181–198.

Riedel CG, Katis VL, Katou Y, Mori S, Itoh T, Helmhart W, Gálová M, Petronczki M, Gregan J, Cetin B, *et al.* Protein phosphatase 2A protects centromeric sister chromatid cohesion during meiosis I. Nature. 2006;441(7089):53–61.

Rockmill B, Roeder GS. Meiosis in asynaptic yeast. Genetics. 1990; 126(3):563–574.

Roeder GS, Bailis JM. The pachytene checkpoint. Trends Genet. 2000; 16(9):395–403.

Rousová D, Nivsarkar V, Altmannova V, Raina VB, Funk SK, Liedtke D, Janning P, Müller F, Reichle H, Vader G, *et al.* Novel mechanistic insights into the role of Mer2 as the keystone of meiotic DNA break formation. Elife. 2021;10:e72330.

Saad H, Gallardo F, Dalvai M, Tanguy-le-Gac N, Lane D, Bystricky K. DNA dynamics during early double-strand break processing revealed by non-intrusive imaging of living cells. PLoS Genet. 2014;10(3):e1004187.

Sanchez A, Adam C, Rauh F, Duroc Y, Ranjha L, Lombard B, Mu X, Wintrebert M, Loew D, Guarné A, *et al.* Exo1 recruits Cdc5 polo kinase to MutLg to ensure efficient meiotic crossover formation. Proc Natl Acad Sci USA. 2020;117(48):30577–30588.

Schindelin J, Arganda-Carreras I, Frise E, Kaynig V, Longair M, Pietzsch T, Preibisch S, Rueden C, Saalfeld S, Schmid B, *et al.* Fiji: an open-source platform for biological-image analysis. Nat Methods. 2012;9(7):676–682.

Schwacha A, Kleckner N. Identification of joint molecules that form frequently between homologs but rarely between sister chromatids during yeast meiosis. Cell. 1994;76(1):51–63.

Schwacha A, Kleckner N. Interhomolog bias during meiotic recombination: meiotic functions promote a highly differentiated interhomolog-only pathway. Cell. 1997;90(6):1123–1135.

Schwartz EK, Wright WD, Ehmsen KT, Evans JE, Stahlberg H, Heyer W-D. Mus81-Mms4 functions as a single heterodimer to cleave nicked intermediates in recombinational DNA repair. Mol Cell Biol. 2012;32(15):3065–3080.

Shimada M, Nabeshima K, Tougan T, Nojima H. The meiotic recombination checkpoint is regulated by checkpoint *rad+* genes in fission yeast. Embo J. 2002;21(11):2807–2818.

Shodhan A, Medhi D, Lichten M. Noncanonical contributions of MutLg to VDE-initiated crossovers during *Saccharomyces cerevisiae* meiosis. G3 (Bethesda). 2019;9(5):1647–1654.

Smagulova F, Gregoretti IV, Brick K, Khil P, Camerini-Otero RD, Petukhova GV. Genome-wide analysis reveals novel molecular features of mouse recombination hotspots. Nature. 2011; 472(7343):375–378.

Smith AV, Roeder GS. The yeast Red1 protein localizes to the cores of meiotic chromosomes. J Cell Biol. 1997;136(5):957–967.

Soh Y-M, Davidson IF, Zamuner S, Basquin J, Bock FP, Taschner M, Veening J-W, De Los Rios P, Peters J-M, Gruber S, *et al.* Self-organization of parS centromeres by the ParB CTP hydrolase. Science. 2019;366(6469):1129–1133.

Sommermeyer V, Beneut C, Chaplais E, Serrentino ME, Borde V. Spp1, a member of the Set1 Complex, promotes meiotic DSB formation in promoters by tethering histone H3K4 methylation sites to chromosome axes. Mol Cell. 2013;49(1):43–54.

Sourirajan A, Lichten M. Polo-like kinase Cdc5 drives exit from pachytene during budding yeast meiosis. Genes Dev. 2008;22(19): 2627–2632.

Srivastava M, Nambiar M, Sharma S, Karki SS, Goldsmith G, Hegde M, Kumar S, Pandey M, Singh RK, Ray P, *et al.* An inhibitor of nonhomologous end-joining abrogates double-strand break repair and impedes cancer progression. Cell. 2012;151(7):1474–1487.

Stanzione M, Baumann M, Papanikos F, Dereli I, Lange J, Ramlal A, Tränkner D, Shibuya H, de Massy B, Watanabe Y, *et al.* Meiotic DNA break formation requires the unsynapsed chromosome axis-binding protein IHO1 (CCDC36) in mice. Nat Cell Biol. 2016; 18(11):1208–1220.

Subramanian VV, MacQueen AJ, Vader G, Shinohara M, Sanchez A, Borde V, Shinohara A, Hochwagen A. Chromosome synapsis alleviates Mek1-dependent suppression of meiotic DNA repair. PLoS Biol. 2016;14(2):e1002369.

Subramanian VV, Zhu X, Markowitz TE, Vale-Silva LA, San-Segundo PA, Hollingsworth NM, Keeney S, Hochwagen A. Persistent DNA-break potential near telomeres increases initiation of meiotic recombination on short chromosomes. Nat Commun. 2019;10(1):970.

Sullivan NL, Marquis KA, Rudner DZ. Recruitment of SMC by ParB-*parS* organizes the origin region and promotes efficient chromosome segregation. Cell. 2009;137(4):697–707.

Sun X, Huang L, Markowitz TE, Blitzblau HG, Chen D, Klein F, Hochwagen A. Transcription dynamically patterns the meiotic chromosome-axis interface. Elife. 2015;4:e07424.

Tesse S, Storlazzi A, Kleckner N, Gargano S, Zickler D. Localization and roles of Ski8p protein in *Sordaria* meiosis and delineation of three mechanistically distinct steps of meiotic homolog juxtaposition. Proc Natl Acad Sci USA. 2003;100(22):12865–12870.

Thacker D, Mohibullah N, Zhu X, Keeney S. Homologue engagement controls meiotic DNA break number and distribution. Nature. 2014;510(7504):241–246.

Thompson DA, Stahl FW. Genetic control of recombination partner preference in yeast meiosis. Isolation and characterization of mutants elevated for meiotic unequal sister-chromatid recombination. Genetics. 1999;153(2):621–641.

Tsubouchi H, Ogawa H. Exo1 roles for repair of DNA double-strand breaks and meiotic crossing over in *Saccharomyces cerevisiae*. Mol Biol Cell. 2000;11(7):2221–2233.

Tsubouchi H, Roeder GS. Budding yeast Hed1 down-regulates the mitotic recombination machinery when meiotic recombination is impaired. Genes Dev. 2006;20(13):1766–1775.

Uetz P, Giot L, Cagney G, Mansfield TA, Judson RS, Knight JR, Lockshon D, Narayan V, Srinivasan M, Pochart P, *et al.* A comprehensive analysis of protein-protein interactions in *Saccharomyces cerevisiae*. Nature. 2000;403(6770):623–627.

Ur SN, Corbett KD. Architecture and dynamics of meiotic chromosomes. Annu Rev Genet. 2021;55:497–526.

van Heemst D, Heyting C. Sister chromatid cohesion and recombination in meiosis. Chromosoma. 2000;109(1–2):10–26.

Walter J-C, Rech J, Walliser N-O, Dorignac J, Geniet F, Palmeri J, Parmeggiani A, Bouet J-Y. Physical modeling of a sliding clamp mechanism for the spreading of ParB at short genomic distance from bacterial centromere sites. iScience. 2020;23(12):101861.

Wang J, Fan HC, Behr B, Quake SR. Genome-wide single-cell analysis of recombination activity and de novo mutation rates in human sperm. Cell. 2012;150(2):402–412.

Wang S, Hassold T, Hunt P, White MA, Zickler D, Kleckner N, Zhang L. Inefficient crossover maturation underlies elevated aneuploidy in human female meiosis. Cell. 2017;168(6):977–989 e917.

Wang TF, Kleckner N, Hunter N. Functional specificity of MutL homologs in yeast: evidence for three Mlh1-based heterocomplexes with distinct roles during meiosis in recombination and mismatch correction. Proc Natl Acad Sci USA. 1999;96(24):13914–13919.

West AM, Rosenberg SC, Ur SN, Lehmer MK, Ye Q, Hagemann G, Caballero I, Usón I, MacQueen AJ, Herzog F, *et al.* A conserved filamentous assembly underlies the structure of the meiotic chromosome axis. Elife. 2019;8:e40372.

West AMV, Komives EA, Corbett KD. Conformational dynamics of the Hop1 HORMA domain reveal a common mechanism with the spindle checkpoint protein Mad2. Nucleic Acids Res. 2018;46(1):279–292.

Whitby MC. Making crossovers during meiosis. Biochem Soc Trans. 2005;33(Pt 6):1451–1455.

Wojtasz L, Daniel K, Roig I, Bolcun-Filas E, Xu H, Boonsanay V, Eckmann CR, Cooke HJ, Jasin M, Keeney S, *et al.* Mouse HORMAD1 and HORMAD2, two conserved meiotic chromosomal proteins, are depleted from synapsed chromosome axes with the help of TRIP13 AAA-ATPase. PLoS Genet. 2009;5(10):e1000702.

Woltering D, Baumgartner B, Bagchi S, Larkin B, Loidl J, de los Santos T, Hollingsworth NM. Meiotic segregation, synapsis, and recombination checkpoint functions require physical interaction between the chromosomal proteins Red1p and Hop1p. Mol Cell Biol. 2000;20(18):6646–6658.

Wu TC, Lichten M. Meiosis-induced double-strand break sites determined by yeast chromatin structure. Science. 1994;263(5146):515–518.

Wu TC, Lichten M. Factors that affect the location and frequency of meiosis-induced double-strand breaks in *Saccharomyces cerevisiae*. Genetics. 1995;140(1):55–66.

Xu L, Ajimura M, Padmore R, Klein C, Kleckner N. *NDT80*, a meiosis-specific gene required for exit from pachytene in *Saccharomyces cerevisiae*. Mol Cell Biol. 1995;15(12):6572–6581.

Xu L, Weiner BM, Kleckner N. Meiotic cells monitor the status of the interhomolog recombination complex. Genes Dev. 1997;11(1):106–118.

Yang F, De La Fuente R, Leu NA, Baumann C, McLaughlin KJ, Wang PJ. Mouse SYCP2 is required for synaptonemal complex assembly and chromosomal synapsis during male meiosis. J Cell Biol. 2006;173(4):497–507.

Yang F, Gell K, van der Heijden GW, Eckardt S, Leu NA, Page DC, Benavente R, Her C, Höög C, McLaughlin KJ, *et al.* Meiotic failure in male mice lacking an X-linked factor. Genes Dev. 2008;22(5):682–691.

Yang S, Yuan Y, Wang L, Li J, Wang W, Liu H, Chen J-Q, Hurst LD, Tian D. Great majority of recombination events in *Arabidopsis* are gene conversion events. Proc Natl Acad Sci USA. 2012;109(51):20992–20997.

Yisehak L, MacQueen AJ. HO endonuclease-initiated recombination in yeast meiosis fails to promote homologous centromere pairing and is not constrained to utilize the Dmc1 recombinase. G3 (Bethesda). 2018;8(11):3637–3659.

Yoon S-W, Lee M-S, Xaver M, Zhang L, Hong S-G, Kong Y-J, Cho H-R, Kleckner N, Kim KP. Meiotic prophase roles of Rec8 in crossover recombination and chromosome structure. Nucleic Acids Res. 2016;44(19):9296–9314.

Youds JL, Boulton SJ. The choice in meiosis - defining the factors that influence crossover or non-crossover formation. J Cell Sci. 2011;124(Pt 4):501–513.

Yue J-X, Li J, Aigrain L, Hallin J, Persson K, Oliver K, Bergström A, Coupland P, Warringer J, Lagomarsino MC, *et al.* Contrasting evolutionary genome dynamics between domesticated and wild yeasts. Nat Genet. 2017;49(6):913–924.

Zakharyevich K, Ma Y, Tang S, Hwang PY-H, Boiteux S, Hunter N. Temporally and biochemically distinct activities of Exo1 during meiosis: double-strand break resection and resolution of double Holliday junctions. Mol Cell. 2010;40(6):1001–1015.

Zakharyevich K, Tang S, Ma Y, Hunter N. Delineation of joint molecule resolution pathways in meiosis identifies a crossover-specific resolvase. Cell. 2012;149(2):334–347.

Zanders S, Alani E. The *pch2*Δ mutation in baker's yeast alters meiotic crossover levels and confers a defect in crossover interference. PLoS Genet. 2009;5(7):e1000571.

Zickler D, Kleckner N. Meiotic chromosomes: integrating structure and function. Annu Rev Genet. 1999;33:603–754.

Zickler D, Kleckner N. Recombination, pairing, and synapsis of homologs during meiosis. Cold Spring Harb Perspect Biol. 2015;7(6):a016626.

Zickler D, Kleckner N. A few of our favorite things: pairing, the bouquet, crossover interference and evolution of meiosis. Semin Cell Dev Biol. 2016;54:135–148.

Communicating editor: A. J. MacQueen